ISTANBUL TECHNICAL UNIVERSITY ★ GRADUATE SCHOOL

ENCAPSULATION OF DRUG INTO BIOPOLYMERIC MATRICES BASED ON MODIFIED XANTHAN GUM AND CHITOSAN MICROPARTICLES

M.Sc. THESIS

Taylan Baran YEŞİL

Departments of Polymer Science & Technology

Polymer Science and Technology Programme

JUNE 2022

ISTANBUL TECHNICAL UNIVERSITY ★ GRADUATE SCHOOL

ENCAPSULATION OF DRUG INTO BIOPOLYMERIC MATRICES BASED ON MODIFIED XANTHAN GUM AND CHITOSAN MICROPARTICLES

M.Sc. THESIS

Taylan Baran YEŞİL
(515191014)

Departments of Polymer Science & Technology

Polymer Science and Technology Programme

Thesis Advisor: Prof. Dr. Orhan GÜNEY

JUNE 2022

İSTANBUL TEKNİK ÜNİVERSİTESİ ★ LİSANSÜSTÜ EĞİTİM ENSTİTÜSÜ

MODİFİYE KSANTAN GAM VE KİTOSAN MİKROPARTİKÜL TEMELLİ BİYOPOLİMERİK MATRİSLERE İLAÇ ENKAPSÜLASYONU

YÜKSEK LİSANS TEZİ

Taylan Baran YEŞİL
(515191014)

Polimer Bilim ve Teknolojisi Anabilim Dalı

Polimer Bilim ve Teknolojisi Programı

Tez Danışmanı: Prof. Dr. Orhan GÜNEY

HAZİRAN 2022

Taylan Baran YESİL, a M.Sc. student of İTU Graduate School student ID 515191014 successfully defended the thesis entitled "ENCAPSULATION OF DRUG INTO BIOPOLYMERIC MATRICES BASED ON MODIFIED XANTHAN GUM AND CHITOSAN MICROPARTICLES", which he prepared after fulfilling the requirements specified in the associated legislations, before the jury whose signatures are below.

Thesis Advisor :	**Prof. Dr. Orhan GUNEY** İstanbul Technical University	.....
Jury Members :	**Prof. Dr. Orhan GUNEY** Istanbul Technical University	.....
	Prof. Dr. Bahire Filiz SENKAL Istanbul Technical University	.....
	Prof. Dr. Cemal OZEROGLU Istanbul University	.....

Date of Submission : 2 June 2022
Date of Defense : 28 June 2022

To my family and friends,

FOREWORD

I would like to thank my advisor Prof. Dr. Orhan GÜNEY for his mentorship and support. During my thesis study, I received too many people's help and support. I felt grateful to have such friends and supervisors who are being there when I needed their support. I have to appreciate Assoc. Prof. Dr. Cem Bülent ÜSTÜNDAĞ and Assoc. Prof. Dr. Oğuzhan GÜNDÜZ for their help with my characterization analyses during my experiments.

I would like to declare my gratitude to my best friends Aşkıcan HACIOĞLU, Arda ÜSTÜN, Hakkı Batu ORDU and my beloved Selin MERCAN for the endless support they provide to me during the writing process of this thesis.

For the ones, I couldn't mention their name here yet have given their hand in this thesis, thank you sincerely.

June 2022

Taylan Baran YEŞİL

(B.Sc. Bioengineer)

TABLE OF CONTENTS

Page

ABBREVIATIONS

DDS **:** Drug Delivery Systems
XG **:** Xanthan Gum
DXG **:** Dialdehyde Xanthan Gum
CH **:** Chitosan
TC **:** *Trans*-cinnamaldehyde
GIT **:** Gastrointestinal Tract
FTIR **:** Fourier Transform Infrared Spectroscopy
DSC **:** Differential Scanning Calorimetry
DLS **:** Dynamic Light Scattering
SEM **:** Scanning Electron Microscope
BBB **:** Blood Brain Barrier
PEG **:** Polyethylene Glycol
PEC **:** Polyelectrolyte Complex
IPNs **:** Interpenatrating Networks
PVA **:** Polyvinyl Alcohol
ECM **:** Extracellular Matrix
PVP **:** Polyvinylpyrrolidone
IG **:** Ionotropic Gelation
NaTPP **:** Sodium Tripolyphosphate
PDI **:** Polydispersity Index
GA **:** Glutaraldehyde
FDA **:** Food and Drug Administration
GRAS **:** Generally Recognized As Safe
PBS **:** Phosphate Buffer Saline
UV **:** Ultraviolet
rpm **:** Revolutions Per Minute
v1 **:** First Version
v2 **:** Final Version
IC **:** Ionic Complex
CC **:** Covalently cross-linked

IC-1 **:** Chitosann-Xanthan gum

IC-2 **:** Chitosan-Xanthan gum-Phosphate

IC-3 **:** Transcinnamaldehyde- Chitosan-Xanthan gum

IC-4 **:** Transcinnamaldehyde-Chitosan-Xanthan gum-Phosphate

CC-1 **:** Chitosan-Dialdehyde-Xanthan gum

CC-2 **:** Chitosan-Dialdehyde Xanthan gum-Phosphate

CC-3 **:** Transcinnamaldehyde-Chitosan-Dialdehyde Xanthan gum

CC-4 **:** Transcinnamaldehyde-Chitosan-Dialdehyde Xanthan gum-Phosphate

SYMBOLS

V	**:** Volume
C	**:** Concentration
m	**:** Weight
MM	**:** Molar Mass
g	**:** Gram
M	**:** Molarity

LIST OF TABLES

Page

LIST OF FIGURES

Page

ENCAPSULATION OF DRUG INTO BIOPOLYMERIC MATRICES BASED ON MODIFIED XANTHAN GUM AND CHITOSAN MICROPARTICLES

SUMMARY

The drug delivery concept is defined as a method of routing a drug or an active compound to achieve a therapeutic effect in the living body. Past a few decades, the scope of drug delivery has been extended due to the improvement in nanotechnology. Nano or micro structures offer superior drug delivery systems (DDSs) for enhanced management and treatment of various diseases. Conventional approaches on drug delivery systems are losing their charm to smart and controlled DDSs which enable reducing applying dosage frequency, less systemic side effects and maintaining sufficient drug concentration in targeted organs. In order to improve the therapeutic effect of active molecules, DDSs are designed to guide them towards to selected region in the body without undesirable side effects. Many polymers have been tailored and used as drug carriers due enhance drug loading, control the drug release, and deliver the drug into the selected area in the body.

Chitosan is a natural cationic polysaccharide obtained by deacetylation of chitin. Chitosan is receiving a lot of interest in the encapsulation of drugs and bioactive compounds due to its biocompatibility, low toxicity and biodegradability. The positive surface charge of chitosan makes it suitable for drug delivery and clinical applications. Crosslinking of chitosan can be delivered by both ionic and covalent cross-linkers. However, due to their toxicity, most chemical cross-linkers described in the literature, such as formaldehyde, glutaraldehyde, glyoxal, and epichlorohydrin, can cause problems in clinical usage.

Xanthan gum (XG) is a negatively charged natural polymer that is produced from a gram-negative bacteria called Xanthomonas campestris via enzymatic biosynthesis. It can be classified as a microbial polysaccharide due to its resource. Important features of xanthan gum are non-toxicity, biocompatibility, remarkable viscosity and swelling properties. Due to its features, XG is widely used in drug delivery, tissue engineering and cosmetic applications.

The anionic nature of XG makes it a good candidate for interacting with positively charged chitosan and forming polyelectrolyte complexes which are widely used in encapsulation or entrapment of natural active molecules such as essential oils.

The aim of this study is to develop and optimize a safe encapsulation system for drug delivery in the human body. *Trans*-cinnamaldehyde (TC) is a natural active molecule extracted from cinnamon oil which is known for its antibacterial and antifungal activity. Like many phytochemicals, TC is also very vulnerable to losing its activity via degradation and volatilization. Encapsulation of TC provides a protection to this active molecule against enzymatic and pH-related degradations and also enhances its chemical stability. Encapsulation of *trans*-cinnamaldehyde with natural polymers and optimizing the release rate of active molecules of the system at different pH values

can be used in controlling human pathogens in the gastrointestinal tract (GIT) without causing toxic effects.

In this thesis, xanthan gum was modified by sodium periodate oxidation and dialdehyde xanthan gum (DXG) was obtained to use as a safe alternative crosslinker for chitosan. Sodium periodate oxidation is an effective method for introducing dialdehyde groups into the polymer backbone since the modification of xanthan gum. This modification involves converting glucopyranose units of xanthan gum to aldehyde and creating extra functional sites for covalent cross-linking. The oxidation procedure of xanthan gum is based on creating C-C cleavage between C2-C3 glucosidic bond by oxidizing hydroxy groups on them in the presence of sodium periodate ($NaIO_4$). This generated cleavage then led to the formation of two aldehyde groups in each oxidized monomeric unit.

Introduced aldehyde groups can react with amine groups of chitosan by Schiff base reaction and form imine bonds. Covalent cross-linking allows chitosan to release less active molecules in acidic pH such as gastric fluid and release more active molecules at neutral pH such as intestinal fluid where it is intended to use.

In this thesis, dialdehyde xanthan gum was synthesized with an oxidization degree of 29.4 %. Microparticles were synthesized by changing the concentrations of DXG while keeping the concentration of chitosan constant and optimized in terms of size, encapsulation efficiency and loading capacity. Obtained microparticles were characterized by FTIR, DSC, SEM and DLS measurements. Release studies of *trans*-cinnamaldehyde loaded microparticles were investigated as a function of pH values in buffer solutions.

Trans-cinnamaldehyde loaded dialdehyde xanthan gum-chitosan microparticles have been shown 80.06 % encapsulation efficiency, over 6.0 μm size with 0.310 PDI value. Loading of *trans*-cinnamaldehyde into synthesized microparticles has been proved via FTIR and DSC analysis. The surface roughness of particles has been demonstrated by SEM analysis. The release profile of synthesized microparticles indicated that the particles showed slower release in acidic conditions and faster release in neutral conditions, compared to its control groups.

MODİFİYE KSANTAN GAM VE KİTOSAN MİKROPARTİKÜL TEMELLİ BİYOPOLİMERİK MATRİSLERE İLAÇ ENKAPSÜLASYONU

ÖZET

İlaç taşıma sistemi tabiri, bir ilacın veya aktif bir bileşiğin canlı vücutta terapötik bir etki elde etmek için yönlendirilme yöntemi olarak tanımlanır. Son birkaç on yılda, nanoteknolojideki gelişmeler nedeniyle ilaç taşıma sistemlerinin kapsadığı alan genişlemiştir. Nano veya mikro yapılar, çeşitli hastalıkların gelişmiş yönetimi ve tedavisi için üstün ilaç dağıtım sistemleri (İTS'ler) sunar. İlaç dağıtım sistemlerine yönelik geleneksel yaklaşımlar, uygulama sıklığını, sistemik yan etkileri azaltan ve hedeflenen organlarda yeterli ilaç konsantrasyonunun korunmasını sağlayan akıllı ve kontrollü İTS'lerle karşılaştırıldığında cazibesini yitirmektedir.

Aktif moleküllerin terapötik etkisini artırmak için İTS'ler, istenmeyen yan etkiler olmadan barındırdığı aktif molekülleri vücutta seçilen bölgeye taşımak için tasarlanmıştır. Birçok polimer, ilaç yüklemesini arttırmak, ilaç salınımını kontrol etmek, ilacı vücutta seçilen bölgeye ulaştırmak gibi olanaklar sunduğu için ilaç taşıyıcı olarak uyarlanmış ve kullanılmıştır.

Polimerik malzemeler ayrıca biyolojik olarak parçalanabilirlikleri, biyouyumlulukları ve tekrarlanabilir üretimleri sayesinde İTS'ler için güçlü adaylar olarak kabul edilmektedir. İlaç taşıma uygulamaları için polimerik taşıyıcılar, ilaç taşınması hedeflenen doku veya organlara bağlı olarak nano veya mikropartiküller, dendrimerler, hidrojeller, miseller, sferoidler, biyokompozitler ve yapı iskeleleri formlarında olabilir.

Kitosan, kitinin deasetilasyonu ile elde edilen doğal bir katyonik polisakkarittir. Bu polimer, biyouyumluluğu, düşük toksisitesi ve biyobozunabilirliği nedeniyle ilaçların ve biyoaktif bileşiklerin kapsüllenmesinde büyük ilgi görmektedir. Kitosanın pozitif yüzey yükü, onu ilaç dağıtımı ve klinik uygulamalar için uygun bir polimer yapmaktadır. Kitosanın çapraz bağlanması, hem iyonik hem de kovalent çapraz bağlayıcılar tarafından sağlanabilir. Ancak kitosanon literatürede çokça çalışılmış olan formaldehit, glutaraldehit, glioksal ve epiklorohidrin gibi çoğu kimyasal çapraz bağlayıcısı toksisiteleri nedeniyle klinik kullanımda sorunlara neden olabilmektedir.

Ksantan gam (KG), Xanthomonas campestris adı verilen gram negatif bir bakteriden enzimatik biyosentez yoluyla üretilen negatif yüklü doğal bir polimerdir. Kaynağından dolayı mikrobiyal polisakkarit olarak sınıflandırılamaktadır. Ksantan gamın önemli özellikleri arasında toksik olmaması, biyouyumluluğu, yüksek viskozitesi ve şişme özellikleri sayılabilir. Bu özellikleri nedeniyle KG, ilaç dağıtımı, doku mühendisliği ve kozmetik uygulamalarda yaygın olarak kullanılmaktadır.

KG'nin anyonik yapısı, bu polimeri pozitif yüklü kitosan ile etkileşime girmek ve uçucu yağlar gibi doğal aktif moleküllerin enkapsülasyonunda yaygın olarak kullanılan polielektrolit kompleksleri oluşturmak için iyi bir aday yapmaktadır.

İnsan patojenleriyle ilgili hastalıkları kontrol etmek için geliştirilen ilaç taşıma sistemleri, etken maddeleri olarak çoğunlukla geleneksel antibiyotikleri kullanır. Ancak son on yılda yapılan çalışmalar, insan patojenlerinin iyi bilinen ve yaygın olarak kullanılan antibiyotiklere karşı direnç kazandığını göstermektedir. Son yıllarda araştırmacılar, bilindik sentetik ilaclara karşı dirençli bakteri suşlarıyla başa çıkmak için sentetik ilaçlara alternatif olarak doğal aktif moleküller üzerinde çalışmaktadır. Bunun sebebi doğal aktif moleküllerin bakteri direncini uyarmadan yüksek antibakteriyel etkinlik gösterebilmesidir.

Bu tez çalışmanın amacı, insan vücudunda ilaç taşınımı için güvenli bir kapsülleme sistemi geliştirmek ve optimize etmektir. *Trans*-sinnamaldehit (TS), yüksek antibakteriyel ve antifungal aktivitesi olduğu bilinen tarçın yağından elde edilen doğal bir aktif moleküldür. Birçok fitokimyasal gibi, TS de bozunma ve buharlaşma yoluyla aktivitesini kaybetmeye çok açıktır. TS'nin kapsüllenmesi, bu aktif moleküle enzimatik ve pH ile ilgili bozulmalara karşı bir koruma sağlar ve ayrıca kimyasal stabilitesini arttırır. *Trans*-sinnamaldehitin doğal polimerlerle enkapsülasyonu ve sistemin aktif moleküllerinin farklı pH'larda salım hızının optimize edilmesi, toksik etkilere neden olmadan gastrointestinal sistemdeki (GİS) insan patojenlerinin kontrolünde kullanılabilir.

Bu tezde, ksantan gam sodyum periyodat oksidasyonu ile modifiye edilmiş ve kitosan için güvenli bir alternatif çapraz bağlayıcı olarak kullanılmak üzere dialdehit ksantan gam (DKG) elde edilmiştir. Sodyum periyodat oksidasyonu, dialdehit gruplarının polimer omurgasına dahil edilmesi için kullanılan etkili bir modifikasyon yöntemdir. Bu modifikasyon, ksantan gamın glukopiranoz birimlerinin aldehite dönüştürülmesini ve kovalent çapraz bağlanma için ekstra fonksiyonel bölgeler yaratılmasını sağlar. Ksantan gamın oksidasyon işlemi, üzerlerindeki hidroksi gruplarının sodyum periyodat ($NaIO_4$) varlığında oksitlenerek C2-C3 glukozidik bağı arasında C-C açıklığı oluşturulmasına dayanır. Oluşan bu bölünme daha sonra oksitlenmiş her monomerik ünitede iki aldehit grubunun oluşmasıyla sonuçlanır.

Eklenen aldehit grupları, kitosanın amin gruplarını Schiff bazı reaksiyonu ile reaksiyona sokabilir ve imin bağları oluşturabilir. Kovalent çapraz bağlama, kitosanın mide sıvısı gibi asidik pH'da daha az aktif moleküller salmasına ve ilaç salımında kullanılması amaçlanan bağırsak sıvısı gibi nötr pH'larda daha fazla aktif molekül salmasına olanak sağlar.

Bu tezde, ksantan gamın sodyum periyodat oksidasyonu üç farklı reaksiyon ve iki farklı reaksiyon bitirme ajanı kullanılarak optimize edilmiştir. Optimize edilen sentezden elde edilen dialdehit ksantan gamın oksidasyon derecesi alkali titrasyon metodu kullanılarak % 29,4 olarak belirlenmiştir. Sentezlenen dialdehit ksantan gamın içerdiği aldehit grupları FTIR analiziyle doğrulanmıştır.

Biyopolimerik matris temelli mikropartikül sentezi sırasında, elde edilen dialdehit ksantan gam farklı konsantrasyonlarda hazırlanıp sabit konsantrasyondaki kitosan ile birleştirilmiştir. Oluşturulan ilaç taşıma sistemi üzerindeki fiziksel etkileşimleri ve çapraz bağlanma etkilerini incelemek için deney düzeneği geniş tutulmuştur. Kontrol grupları ile TS yüklü kitosan-dialdehit ksantan gam ve kitosan- ksantan gam mikropartiküllerinin sentezi yapılmıştır. Ayrıca sentezlenen partiküller boyut, kapsülleme verimliliği ve yükleme kapasitesi açısından değerlendirildi ve sentez metodu buna göre optimize edilmiştir.

Elde edilen mikropartiküller FTIR, DSC, SEM ve DLS analizleri ile karakterize edilmiştir. *Trans*-sinnamaldehit yüklü mikropartiküllerin salım çalışmaları, tampon

çözeltilerdeki pH değerlerinin bir fonksiyonu olarak araştırıldı. Tampon çözeltiler pH 2 ve 7'de hazırlanmış ve sentezlenen partiküller her iki pH için de salım deneyine tabii tutulmuştur. Asidik ve nötral pH'larda hazırlanan salım tamponlarının amacı gastrointestinal sistemdeki pH değerlerini stimüle etmek içindir.

Trans-sinnamaldehit yüklü dialdehit ksantan gam-kitosan mikropartikülleri, DLS analizi sonucunda 0,31 PDI değeri ile 6 µm üzerinde partikül çapına sahip olduğunu göstermiştir. Mikropartiküllerin kapsülleme verimliliği % 80,06 olarak belirlenmiş ve partiküllerin yüklenme kapasitesinin % 43,57 olduğu, yüklenen aktif molekülün kuru kapsül ağırlığına oranlanması ile tespit edilmiştir.

Sentezlenmiş partiküllere *trans*-sinnamaldehitin yüklendiğinin doğrulanması, FTIR ve DSC analizleri ile sağlanmıştır. Parçacıkların yüzey morfolojisi SEM analizi ile gerçekleştirilmiş ve partikül yüzey pürüzlülüğü incelenmiştir. *Trans*-sinnamaldehit yüklü dialdehit ksantan gam-kitosan mikropartiküllerinin salım profili, kontrol gruplarına kıyasla, partiküllerin asidik ortamda daha az salım yaparken nötral koşullarda daha fazla salım yaptığını göstermiştir.

1. INTRODUCTION

1.1 Drug Delivery Systems

The drug delivery concept is defined as the method of routing a drug or an active compound to achieve a therapeutic effect in the living body [1]. Past a few decades, the scope of drug delivery has been extended due to the improvement in nanotechnology. Thanks to nanotechnology, alteration of characteristics of materials and production of nano or micro structures become more easy. Nano or micro structures offer superior drug delivery systems (DDSs) for enhanced management and treatment of various diseases [2]. Conventional approaches on DDSs are losing their charm to smart and controlled DDSs which enable reducing applying dosage frequency, less systemic side effects and maintaining sufficient drug concentration in targeted organs [3]. In order to improve the therapeutic effect of active molecules, DDSs are designed to guide them towards to selected region in the body without undesirable side effects. Many polymers, lipids and inorganic materials have been tailored and used as drug carriers. The main reasons behind the using these carriers are to enhance drug loading capacity, control the drug release and deliver the drug into the selected area in the body [3-5].

In general, different types of drugs or active molecules are treated with inert compounds to formulate dosage forms called excipients. These excipients are used for enhancing the bioavailability of drugs and regulating drug dosage forms. Excipients can include stabilizers, thickeners, matrix forming agents, release retardants, coating agents, mucoadhesive agents, emulsifiers [6]. Due to the inert nature of these excipients, they cannot play a role in a therapeutic manner or cannot alter the biological action of drugs. However, these excipients can have an effect on the release rate and extent of drug absorption [7] .

Compared to other drug carrier materials, polymers, including natural, semi-natural and synthetic polymers, provide countless opportunities to modulate the properties of

drug delivery systems. Polymeric materials can be also strong candidates for DDSs in terms of their biodegradability, biocompatibility, and reproducibility features [8].

Polymeric carriers for drug delivery applications can be contained nano or microparticles, microcapsules, beads, dendrimers, gels, hydrogels, micelles, spheroids, biocomposites, scaffolds depending on the targeted tissue or organs as shown in Figure 1.1.

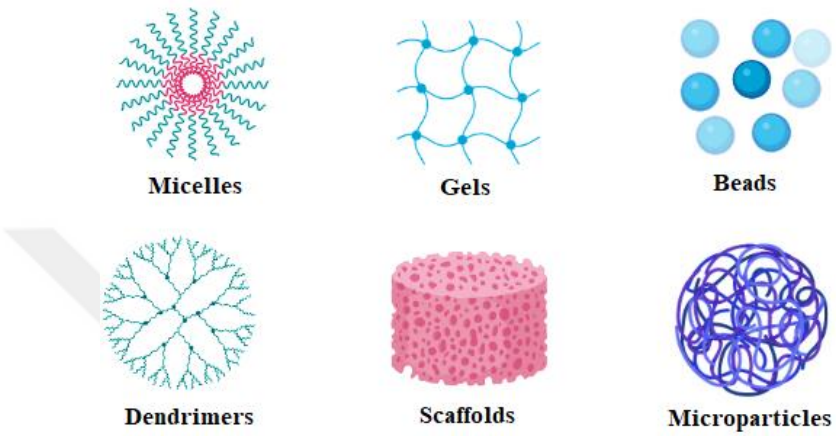

Figure 1.1 : Various drug delivery systems.

Natural and synthetic polymers can be utilized in drug delivery systems. However, natural polymers are more favorable compared to the synthetic polymers because they tend to chemical modification, renewable, cheap, non-toxic, stable, hydrophilic, biodegradable, and biocompatible compared to expensive synthetic polymers that have shown toxicity problems [9]. One of the most intriguing natural polymer class is biopolymers. Polysaccharides are natural biopolymers which have great attraction as useful materials in a number of biomedical fields. Polysaccharides have several functional groups, and thanks to these functional groups, they exhibit tunable physicochemical properties and essential biological activities that make them suitable materials in many pharmaceutical fields such as drug delivery applications [9].

Accurate selection of a polymer or polymers in biopolymer made DDS is still remaining as a challenge for researchers. One of the primary goals of using biopolymeric materials as drug carriers is to protect the drug from degradation or getting damaged besides delivering the drug to the desired site of the body without causing toxicity [7]. However, depending on the selected drug carrier, release rate and intended release environment of loaded drug and the size of the system can be specialized as required. In clinical aspect, the size of the designed system is crucial in

terms of delivering or penetrating intended organ, tissue or cell [10]. The length scale to be considered when designing a drug delivery system is shown in general in Figure 1.2.

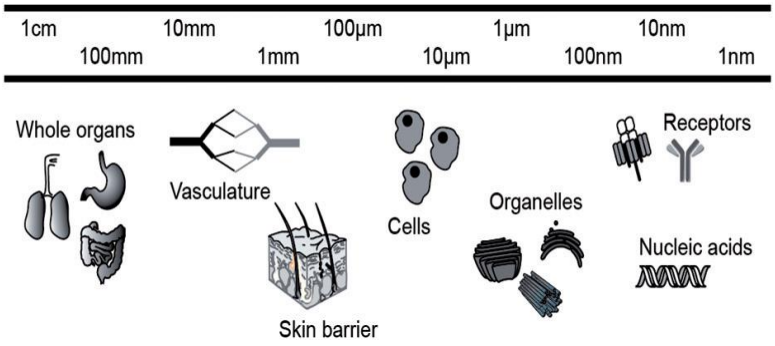

Figure 1.2 : Length scales in drug delivery. Adapted from Delcassian, Patel [10].

1.1.1 Polymeric nanocarriers for drug delivery

1.1.1.1 Polymeric micelles

Polymeric micelles are core-shell structures which are occurred by the self association of amphiphilic block copolymers when they contact with an aqueous solvent [11]. Polymeric micelles, known as nano-sized molecules, are used in drug delivery due to their biocompatibility, low toxicity and morphologic features. Their core-shell structure enables them to carry hydrophobic drugs in the hydrophobic core region while their hydrophilic shell stabilizes the core in an aqueous medium and elevates the water solubility of the polymer [12]. Thanks to these features, polymeric micelles are widely used in various clinical applications such as cancer treatment, estrogen therapy and antiviral therapy [11]. Preparation techniques for polymeric micelles include direct dissolution, dialysis or solvent casting [13]. Diblock copolymers, such as poly(ethylene glycol) (PEG); triblock copolymers, such as poly(ethylene oxide); and graft copolymers such as stearic acid and G-chitosan can be employed in preparation of polymeric micelles [11].

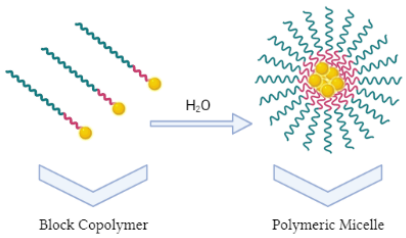

Figure 1.3 : Polymeric micelle formation from block copolymers.

The interaction type of carried drug with polymeric micelles can be chemical or physical. Chemical type includes covalent interactions between drug and structure which are considered more stable than physical type.

1.1.1.2 Polymeric nanoparticles

Solid colloidal particles with a size range between 10 to 1000 nm are classified as polymeric nanoparticles. They can be made of biocompatible and biodegradable polymers in which an active molecule or drug is entrapped within the carrier, adsorbed on the carrier or chemically linked to the surface of the carrier [11, 14]. Nanoparticle term refers to both reservoir based systems called nanocapsules and matrix based systems called nanospheres [14]. Identification of these subclasses is made by their morphological characteristics as shown in Figure 1.4.

Polymeric nanoparticles offer water solubility, nontoxicity, longer shelf life and stability during storage. Thanks to these features, polymeric nanoparticles play an important role in delivering drugs, proteins and genes to targeted tissue or organs. Therefore polymeric nanoparticles are used in clinical fields such as anticancer therapy, gene therapy, crossing the blood-brain barrier (BBB) [11].

Polymeric nanoparticles can be produced by dispersion technique which includes; solvent evaporation, salting out, supercritical fluid, nanoprecipitation, dialysis and emulsification methods.

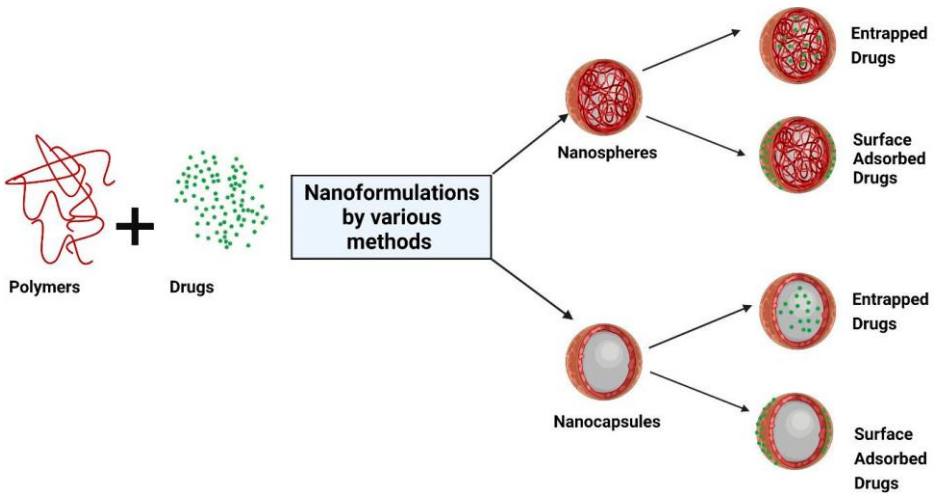

Figure 1.4 : Structures of nanocapsules and nanospheres. Adapted from Procopio, Lagreca [14].

They can also be produced by polymerization of monomers which includes; emulsion, microemulsion, interfacial polymerization and living radical polymerization techniques. Finally, polymeric nanoparticles will be obtained from hydrophilic polymers, ionic gelation and coacervation techniques can be used for synthesis [11, 15].

Natural hydrophilic polymers such as gelatin, albumin, alginate, chitosan and synthetic hydrophobic polymers such as polystyrene, poly(ε-caprolactone), poly(methyl methacrylate) can be used in the preparation of polymeric nanoparticles [16].

1.1.1.3 Dendrimers

Dendrimers are considered a relatively new class of polymeric material. They are tree-shaped macromolecules, generally up to 10 nm in size, which branch out from the center of the structure [2, 17]. Branched structure, multivalency, controllable molecular weight and surface functionality of dendrimers attract researchers' attention to using dendrimers as carriers for drug delivery applications. Their spherically shaped structure consists of internal cavities which enable the drug to be encapsulated within the interior of dendrimers [2]. Controlled release behaviour of the encapsulated drug within the core of this structure has been reported [18]. However, the drug cannot just be encapsulated in the core or also can be attached on the surface of dendrimers as shown in Figure 1.5.

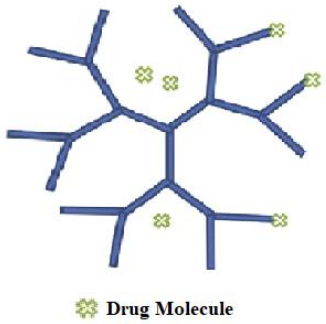

Figure 1.5 : Representaion of a drug molecule encapsulated in dendrimer, adapted and modified from Yadav, Almokdad [11].

Both hydrophobic and hydrophilic drugs can be carried with dendrimers thanks to their versatility [2]. They exhibit valuable actions such as increasing the solubility of non-soluble drugs, elevating the circulation of the drugs in the body.

During the preparation of dendrimers, three strategies can be followed, which are divergent, convergent and both previous strategies at the same time.

In the divergent method, the growth of dendrimers is started from the central core and branches are extending towards the surface. Purification of the final product has been challenging for this approach due to the great amount of dendrimers obtained [19].

In the convergent method, unlike the divergent method, dendrimers start to grow from the end of the branches and extend inwards to form inner core of the structure. The purification step is relatively easy for this method comparing the divergent method [11].

In the final strategy, exponential and mixed growth approaches of the abovementioned methods take place. Basically, two monomers are prepared by using divergent and convergent methods and reacted together to form a trimer which can be used to repeat the growth process [11].

The main drawbacks of dendrimers can be listed as their requirement for multi-step production process and low entrapment efficiency of considerably large drug molecules [20].

1.1.2 Biopolymeric network based drug delivery

Nowadays, novel drug delivery approaches that employ natural polymers such as carbohydrates and proteins has been escalating due to their sustainability, biodegradability and biocompatibility features compared to synthetic polymers. Natural polymers are also cheaper thanks to they are obtained from natural resources [21]. A polymer matrice can be designed with single or multiple polymers. Recent studies indicate that polymer matrices designed with a single biopolymer have troubles in terms of mechanical strength, swelling properties and hydration problems [21, 22]. In order to overcome these problems, biopolymeric matrices made of a single biopolymer can be integrated with second or multiple biomaterials, such as carbohydrates and proteins. This integration can also include bioceramics and synthetic polymers. Strategies that can be applied while handling with abovementioned troubles are chemical modifications such as esterification, carboxymethylation, graft co-polymerization, cross-linking, polyelectrolyte complexation (PEC) and interpenetrating polymeric networks (IPNs) [21]. Thanks to

these modifications, natural polymers can be used for site specific delivery while overcoming single polymer related drawbacks. IPNs are coming forward as a functional method which enhanced the properties and performance of natural polymers.

Natural polymers can be physically cross-linked, chemically cross-linked or both chemically and physically cross-linked at the same time to form IPNs [23]. Depending on the chemical bonds of IPNs consist, they can be categorized as covalent IPNs and non-covalent IPNs. Non-covalent IPNs are divided into two categories which are non-covalent full IPNs and non-covalent semi-IPNs as shown in Figure 1.6.

Covalent IPNs are polymer structures consist two polymers which are covalently cross-linked unlike single polymeric networks [21, 24].

Non-covalent full IPNs are also polymer structures consist two polymers, however, both of these two polymers are independently cross-linked apart from covalent cross-linking. In the non-covalent semi IPNs, one of the polymers is cross-linked without covalent interaction [21].

IPNs provide unique features of constituted two polymers. The superior side of IPNs over polymer blends is that IPNs can display different functional characteristics and performance due to two or more polymers comprised in one system.

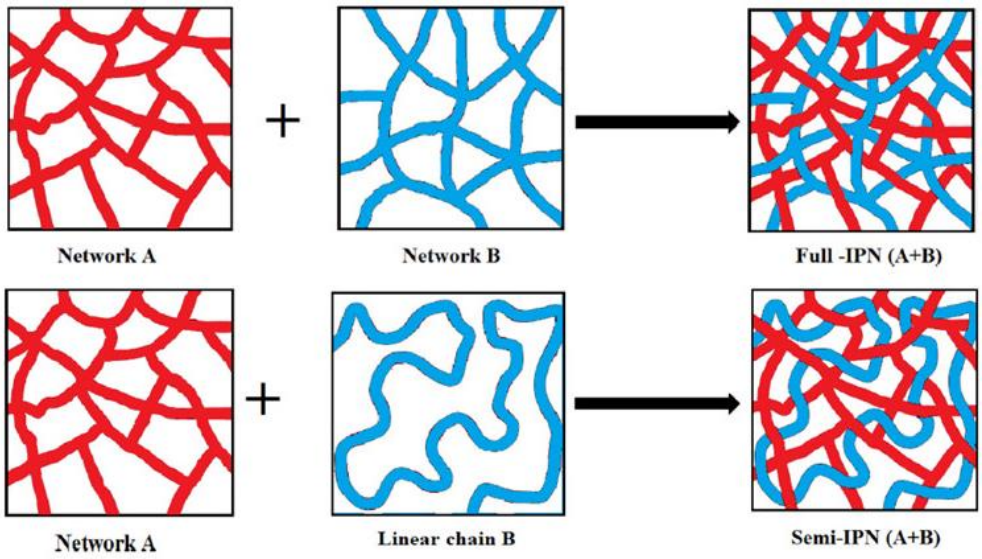

Figure 1.6 : Schematic represantation of full and semi IPNs. Adapted from Farooq, Teuwen [25].

IPNs composed of two or more polymeric networks are in some way interlaced at least to some degree at the molecular level but do not interact chemically with one another. These polymers cannot be disassembled from each other as long as the chemical bond is maintained [21]. Thanks to the abovementioned characteristics, IPNs are separated from the block- and graft-copolymers and polymer blends. They have good swelling capabilities without degradation or dissolving is another significant property of IPNs which makes them valuable for drug delivery systems [21]. Tunable swelling behaviour of IPNs also makes them more preferable over PECs, which can swell uncontrollably and eventually dissolve and degrade in aqueous media due to their physically cross-linked structures which exhibit low shear strength and tensile strength for hydrogel versions [26].

Hydrogels are simply hydrophilic structure networks which can be formed either physically or chemically via cross-linking of their polymer chains. Result of this cross-linking, polymer chains of hydrogel has formed network that can be consisted of hydrogen bonds, covalent bonds, Van der Waals interactions and physical entanglings [27].

IPN systems employ numerous natural polymers and biopolymers such as chitosan, alginate, pectin, cellulose, guar gum, gellan gum, xanthan gum, locuts bean gum, starch, carrageenan, dextran, hyaluronic acid. For the past decade, researchers have been working on IPNs which include one or more abovementioned polymers, their cross-linkers and modified versions of these polymers to produce drug delivery carriers.

To give examples from the studies has been accomplished in the past years, chitosan and tamarind seed polysaccharide microparticles were produced by using the IPN system and glutaraldehyde in Jana, Saha [28] study. In this study, covalent cross-linking delivered by glutaraldehyde and aceclofenac was encapsulated with an encapsulation efficiency over 85 %. The spherical shape of obtained microparticles was confirmed with scanning electron microscopy (SEM) analysis and IPN formation between chitosan and tamarind seed polysaccharide was also confirmed by Fourier transform-infrared (FTIR) analysis. In another study of the same researchers, sustained release of aceclofenac was observed from compressed chitosan-tamarind seed polysaccharide in matrix tablet for over eight hours [29].

In Bulut [30] study, ibuprofen loaded chitosan/poly(vinyl alcohol) (PVA) IPN microspheres were produced with the help of the water-in-oil emulsification technique. Glutaraldehyde was also used as a covalent cross-linker in this study. A significant finding in this study is that the release behaviour of ibuprofen tends to get slower as the degree of cross-linking increases.

Xinxin, Zhang [31] reported that doxorubicin loaded IPN microspheres using chitosan and poly (2-acrylamide-2-methylpropanesulfonic acid) (PAMPS) exhibited improved loading of the drug compared to raw chitosan microspheres. They also emphasized that during cytotoxicity evaluation, they observed over 90% cell viability of 3T3 cell and HeLa cells which is the evidence of biocompatibility of created IPN microsphere system.

Ullah, Javed [32] formulated a chemically cross-linked IPN system which includes functionalized chitosan-alginic acid for poorly soluble drugs. In this study, polymers were functionalized by co-polymerization and hydroxyl groups of alginic acid were replaced with 4-aminophenol and 1,2-ethyleneamide. Due to electrostatic complexation provided by hydrophilic ligands with aqueous drug solutions, IPN formulation showed extended drug release of poorly soluble drugs *in vitro*.

In Puertas-Bartolomé, Benito-Garzón [33] work, catechol loaded IPN based hydrogel was synthesized by using chitosan and oxidized hyaluronic acid. IPNs were produced with the help of self covalent cross-linking mechanism between chitosan and oxidized hyaluronic acid in the presence of catechol terpolymer which was co-ordinated to iron to form IPN structure. Obtained IPN was considered a candidate for wound dressing material due to its extracellular matrix (ECM) mimicking properties.

In a study by Anwar, Pervaiz [34], 5-fluorouracil loaded IPN hydrogels were formulated for colon-specific delivery. Novel types of xanthan gum and polyvinylpyrrolidone (PVP) were crosslinked chemically via free radical polymerization with a presence of monomer to obtain xanthan gum-PVP-co-poly acrylic acid IPN hydrogels. Ethylene glycol dimethacrylate was used as a cross-linker for this system. pH-responsive behaviour of created IPNs was determined by release studies conducted in the simulated gastrointestinal fluids medium.

In another study, Ray, Banerjee [35] produced pH-responsive microspheres by using xanhan gum and PVA based IPN system for intestinal drug delivery. They loaded

these microspheres with diclofenac sodium and cross-linked this system with glutaraldehyde. Their work demonstrated that, in vitro drug release pattern of the system is highly dependent on xanthan gum-PVA ratio.

1.1.3 Polymeric particle synthesis methodologies

Production methods of nano-sized or micro-sized polymeric particles have been limited due to their complexities. Researchers have been suffering from the disadvantages of conventional particle production methods in terms of their high cost, long synthesis time, re-producibility problems.

Over time, numerous polymer and preparation methods have been developed and applied for the encapsulation of active molecules; however, there is no single encapsulation method which can fulfil all the requirements for all active molecules to be encapsulated in all product applications. Depending on the particle synthesis method, particles will have different sizes, shapes and morphology. The wise selection of synthesis method and polymer for an involved active molecule is crucial for controlling the functional properties of the final product.

Polymeric nano- or micro-particle preparation methods generally consist of two main steps; preparation of the emulsification system and precipitation or gelation of the polymer [20].

1.1.3.1 Ionotropic gelation

Ionotropic gelation relies on the ability of polyelectrolytes to cross-link when counterions are present [36]. Ionotropic gelation (IG) method includes two sub-groups which are internal and external. These two approaches differ from each other by the position of cross-linker counterion. In external IG, a cross-linker counterion is installed externally into the system. In internal IG, a cross-linking counterion is integrated into the polymer solution.

Advantages of external cross-linked particles can be listed as higher matrix strength, relatively higher encapsulation efficiency and more controller release of active molecules [37]. The IG method does not require expensive equipment or expensive reagents, and the active molecule can be encapsulated in a short period of time [38]. PEC technique can also be applied to polymers which are used in IG methods to

enhance the quality and mechanical properties of synthesized beads synergically [39].

Chitosan, a cationic biopolymer, can be physically cross-linked by anionic sodium-tri-polyphosphate (NaTPP) in an acidic medium. There are plenty of studies that involve chitosan and IG method in the literature. For instance, Wu, Wang [40] used this mechanism in their study to obtain resveratrol loaded chitosan nanoparticles.

1.1.3.2 Polyelectrolyte complexation

Polyelectrolyte complexation method relies on electrostatic interactions between oppositely charged polymers. These interactions can be resulted in the formation of polyelectrolyte complexes (PECs) to become hydrogels or polymeric aggregates as a final product [26, 41]. The size range of the particles obtained from PEC method can vary from nanometer to micrometer. Polysaccharides such as anionic alginate and cationic chitosan are favorable polymers for this method due to their hydrophilic and biocompatible properties [42]. The stability and mechnanical properties of PECs are limited due to their electrostatic interactions.

1.1.3.3 Ionotropic gelation polyelectrolyte complexation

This method is basically applying the abovementioned two strategies in one particle production system. Counterions in the system promote cross-linking of polyelectrolytes to form hydrogels or particles which will precipitate [41]. Polysaccharides that are generally utilized in such systems can be dissolved in an acidic environment to create ionic solutions. The created ionic solution is firstly cross-linked with its counterion to form a hydrogel in the IG step. Then, the formed hydrogel is treated with an aqueous solution of polyvalent counterions to form PEC.

A cationic polymer such as chitosan and anionic polysaccharides and their ionic cross-linkers (NaTPP, CaCl2, etc.) are vastly studied in this method due to their charge and non-toxic biocompatible features..

1.1.3.4 Complex coacervation

According to IUPAC, coacervation is the phase separation of colloidal systems into two liquid phases. One phase is more concentrated with a colloid component inside called coacervate while the other phase is equilibrium solution. The coacervation

concept can be investigated under two groups called simple and complex coacervation [43].

Complex coacervation is a type of coacervation which involves two oppositely charged polyelectrolytes. In simple coacervation, the system consists of one colloidal solute. In complex coacervation, the role of pH of oppositely charged polyelectrolytes is critical. In order to form coacervates from the complex coacervation method, pH has to be adjusted to a point where the oppositely charged polymers have maximum ion concentration in the solution [43]. Coacervates are formed as a result of salt bonding and electrostatic interactions between two polymer solutions whereas ionic gelation is occurred from liquid to gel due to ionic interactions as shown in Figure 1.7.

Another explanation for complex coacervation is that the method involves liquid-liquid phase separation of two oppositely charged polyelectrolytes under a suitable pH range to form enclosed solid particles called coacervates [16, 43].

The complex coacervation method is widely used to encapsulate poorly water soluble active molecules due to the formation of particles is mostly involved hydrophobic forces with high encapsulation efficiency [43-45].

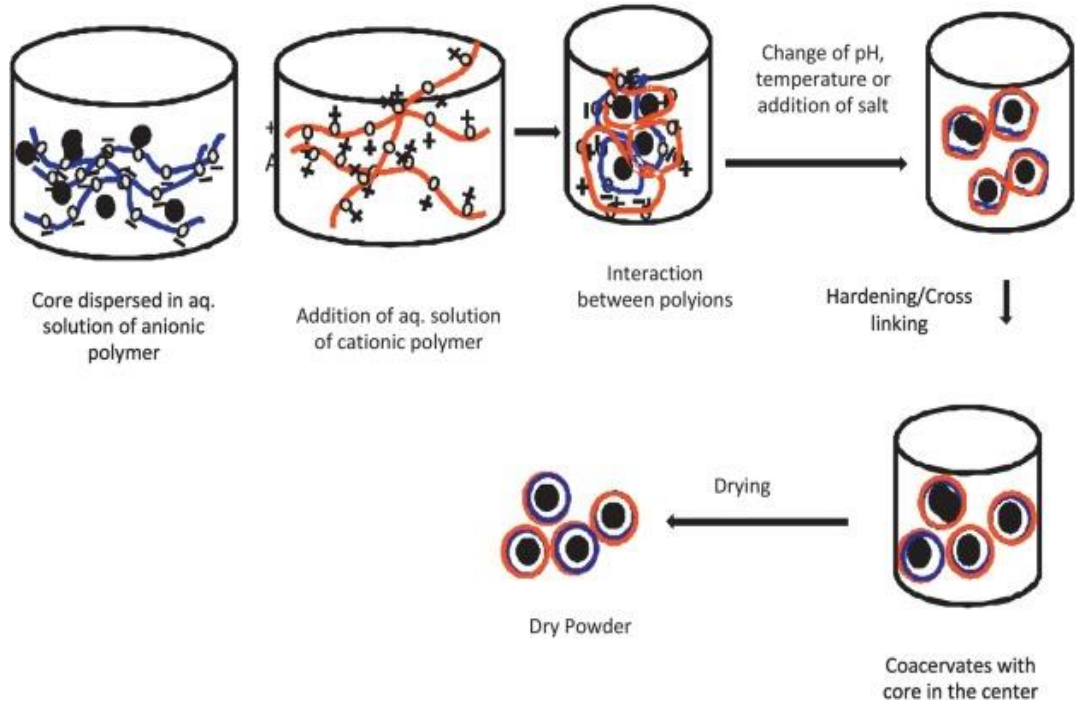

Figure 1.7 : Schematic representation of complex coacervation. Adapted from Timilsena, Akanbi [46].

1.1.3.5 Emulsification solvent evaporation

The emulsification solvent evaporation method consists of volatile solvents to be used to dissolve polymer and form emulsions with various stabilizers eventually. These solvents may include chloroform, acetone, dichloromethane. As it is shown in Figure 1.8, nanoparticles can be formed via evaporation of volatile solvent through the diffusion of continuous phase of the emulsion [20].

The main advantages of this method are high encapsulation efficiency, smaller particle size and process re-producibility, convenience of lipophilic active molecule encapsulation. However during this emulsification process, high energy consuming homogenization methods and hazardous chemical solvents are required [16].

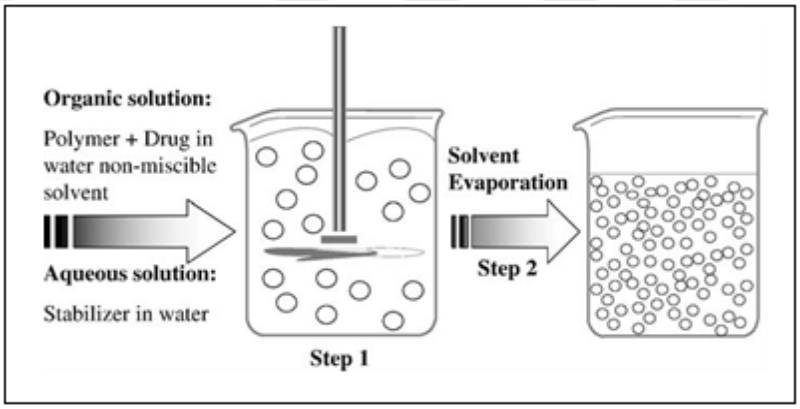

Figure 1.8 : Schematic representation of solvent evaporation method. Adapted from Reis, Neufeld [47].

1.1.3.6 Emulsification solvent diffusion

The emulsification solvent diffusion method can be considered a modified version of the solvent evaporation method. The polymer used in this method is dissolved in a partially water soluble solvent like propylene carbonate and then saturated with water to reach the thermodynamic equilibrium state of liquids [16].

In order to obtain nanoparticles, this phase is emulsified in an aqueous solution which consists of stabilizers to induce solvent diffusion to the external phase as shown in Figure 1.9.

The elimination step of solvent can be delivered by evaporation or filtration. The solvent transport step creates physicochemical instability in the system which leads to forming of nanoparticles [16].

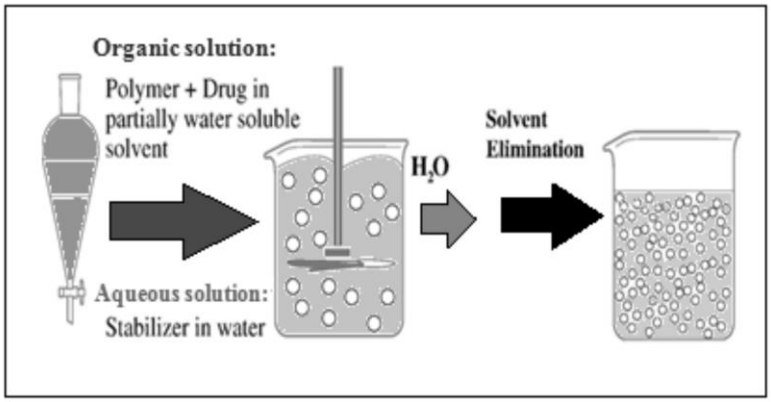

Figure 1.9 : Schematic representation of emulsification solvent evaporation. Adapted from Nagavarma, Yadav [16].

This method offers high encapsulation efficiency, no requirement for homogenization and small sized particles with low PDI value. However, requirement of removing elevated volumes of water from the system and non-convenience for water soluble active molecule encapsulation are drawbacks of solvent diffusion method [47].

1.1.3.7 Salting out

The salting out method is considered a modification of the solvent diffusion method. Basically, the salting out effect serves as a separator of water miscible solvent from water based solution [16]. In this method, water-miscible solvent like acetone is used to dissolve the polymer and active molecule. The prepared solution is emulsified in an aqueous gel with stabilizers, then the salting out effect which is provided by electrolytes, separates acetone from the aqueous solution.

Electrolyte based salting out agents may include magnesium chloride, magnesium acetate and calcium chloride [16]. Determination of the agent for salting out is critical for the process due to its control over the encapsulation efficiency of the active molecule to be encapsulated.

The final emulsion is diluted with water to induce acetone to diffuse into the water phase. Thanks to the diffusion of acetone, polymer aggregation occurs as shown in Figure 1.10. Nanoparticles are obtained from these aggregates.

The main drawbacks of salting out method are that it is only used to encapsulate lipophilic drugs and proteins and it requires extensive purification to eliminate salting agent used in the process [16, 48].

Figure 1.10 : Schematic representation of salting out method. Adapted from Dubey, Mody [48].

1.1.3.8 Nanoprecipitation

The nanoprecipitation method is basically a method that involves solvent displacement. In this method, a polymer is dissolved in an organic solvent with an active molecule and surfactant. Then this solution is transferred into an aqueous medium which enables organic solvent to diffuse through to water and precipitation of its dissolved polymer [16]. Nanoparticles are generated from this precipitation, after the precipitation of polymer, a vacuum can be used to evaporate the organic solvent from the system as represented in Figure 1.11.

Stabilizers and surfactants are also used in the aqueous medium where nanoprecipitation takes place. They have an important role in controlling the size, stability and surface properties of nanoprecipitate particles [49].

Nanoprecipitation can be considered as no homogenization required simple method, it has drawbacks such as limited water-miscible solvent options and low encapsulation efficiency of water soluble drugs [16].

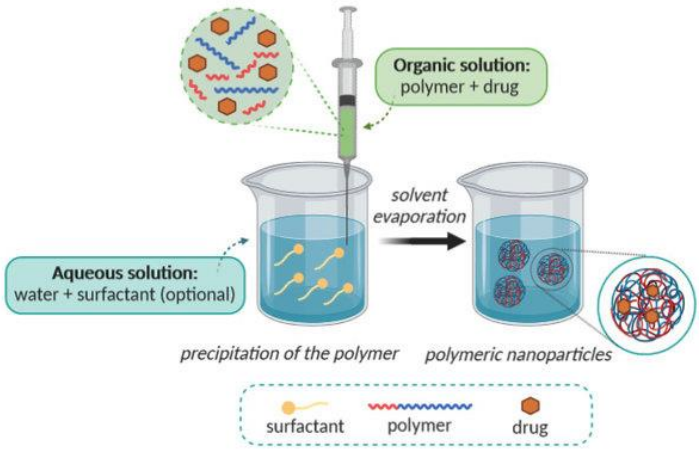

Figure 1.11 : Schematic representation of nanoprecipitation. Adapted from Zielińska, Carreiró [49].

1.2 Assembly Components of Modified Xanthan Gum-Chitosan Microparticles

In this section, detailed information is given about chitosan, xanthan gum, dialdehyde xanthan gum and *trans*-cinnamaldehyde which are the main assembly components of microparticles synthesized in this thesis.

1.2.1 Chitosan

Chitosan can be defined as a cationic polysaccharide which made up of the random distribution of β (1→4) linked 2- amino- 2- deoxy- D- glucose (D-glucosamine) and 2- acetamido- 2- deoxy- D- glucose (N- acetyl- D- glucosamine) units. Chitosan is obtained by deacetylation of chitin which is mostly found in crustacean shells [50, 51].

Chitin can be obtained from numerous natural sources such as fungi, exoskeletons of anthropods, lobsters, shrimps and insects. However, the main source of chitin is provided by crustacean shells due to their low cost and high chitin content [50].

The deacetylation process to obtain chitosan from chitin is generally delivered by hydrolysis under alkali conditions at high temperatures as shown in Figures 1.12 and 1.13. There are four steps involved processes of chitin to obtain chitosan which are deproteinization, demineralization, decoloration and deacetylation [50].

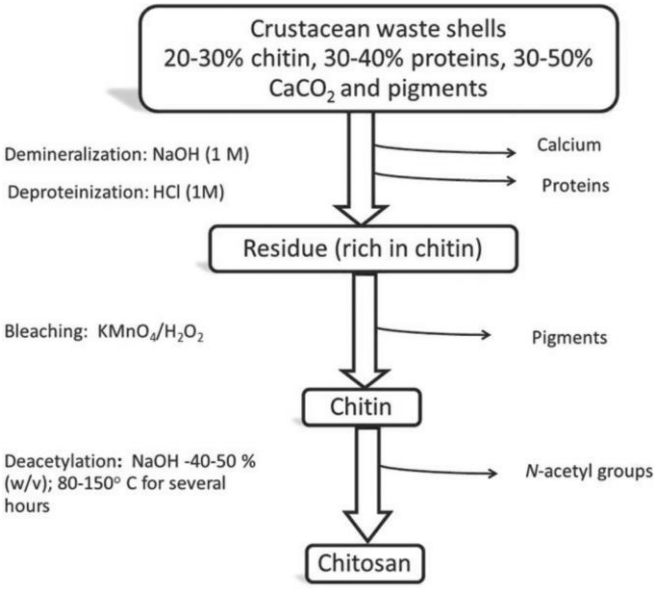

Figure 1.12 : Deacetylation procedure of chitin from crustacean shells. Adapted from Kaur and Dhillon [52].

Primary amino groups found in the chitosan backbone determines the degree of deacetylation and molecular weight of obtained chitosan [53].

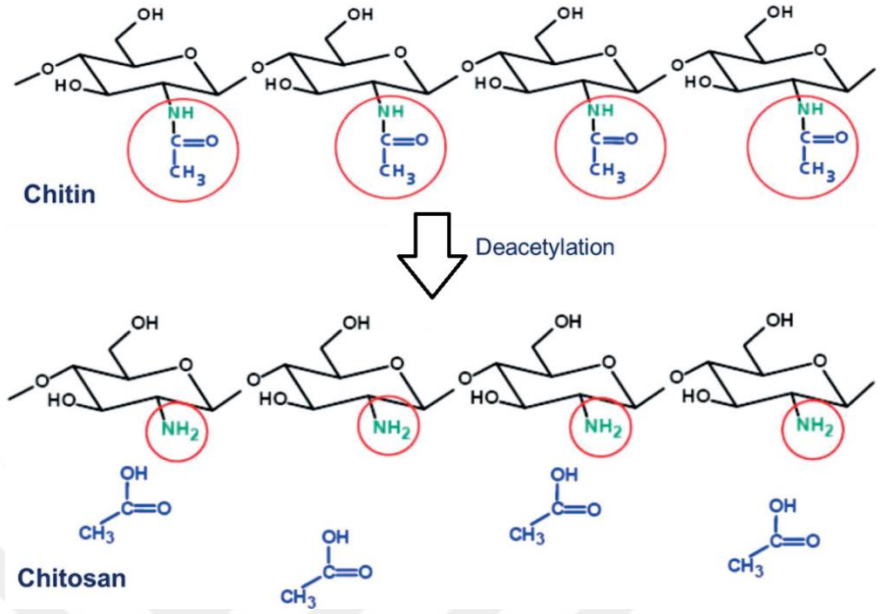

Figure 1.13 : Structure of chitin and chitosan. Adapted from Kaur and Dhillon [52].

Based on their chemical characteristics, chitosan-based products have been enhanced in the last couple of years. Chitosan is mostly soluble in an acidic medium which is basically below pH 6. Because of its amine groups, it is a weak base and its pKa is equal to 6.3. Amine groups can be charged positively at low pH due to protonation. This way it can be a water-soluble-cationic polyelectrolyte. On the other hand, above pH 6, amine groups can be deprotonated which leads to losing its charges. In the end, the polymer transforms from soluble to insoluble [54].

One and only poly-cation on earth is chitosan. Acetylation degree and pH of the medium can vary the charge density of chitosan [55]. The solubility of chitosan is affected by its molecular weight and degree of acetylation.

On the other side, high molecular weight chitosan is soluble only in an acidic medium. If chitosan could have occurred from the high amount of deacetylation degree, it can only be soluble in an acidic medium. Its pH property lacks the usage of chitosan in some applications. Because of this characteristic property, improved soluble derivatives have been synthesized [51]. Some of the concern areas identified include the polymer modification to widen their usage; information on the mechanisms involved in the biological activity of chitosan and chitosan derivatives [56].

1.2.1.1 Chemistry of chitosan

Chitosan (CH) can be classified as a biopolymer due to its biological resources. Biocompatibility, biodegradability, non-toxicity and antimicrobial activity are valuable features of chitosan [57]. Most of its features are highly dependent on the physicochemical properties of chitosan [55]. The acetylation degree and molecular weight of chitosan determine most of the physicochemical properties of this biopolymer.

As shown in Figure 1.14, the reactive groups found in chitosan are the amino ($-NH_2$) group and hydroxyl (-OH) groups. Glycosidic bonds and the acetamide group can be included in functional groups of chitosan [55]. These functional groups can make an opportunity for many modifications which allow chitosan to gain new properties such as solubility as a function of final applications [58].

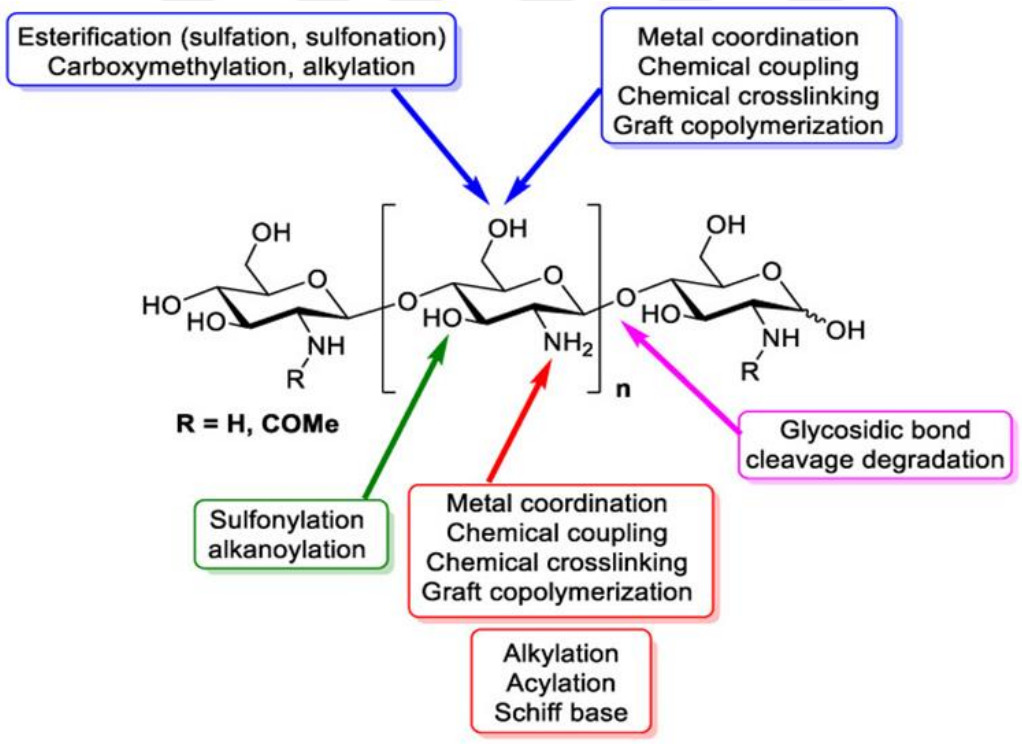

Figure 1.14 : Chemically modifiable functional groups in structure of chitosan. Adapted from Aranaz, Alcántara [55].

Amine and hydroxyl groups of chitosan provide interesting applications to this polymer, since these can be modified to enhance some of the features of this biopolymer. Chemical processes such as; cross-linking, graft copolymerization,

carboxymethylation, etherification, and esterification are widely employed methods to functionalize the chitosan structure [55, 59].

1.2.1.2 Cross-linking mechanisms of chitosan

Cross-linking of chitosan generally needs specific chemical agents to link the polymer chains together and form a 3D macromolecular network. Chitosan can be cross-linked by either covalent or ionic interactions. In order to cross-link chitosan with covalent bonds, aldehyde derivatives are widely used such as glutaraldehyde, glyoxal and formaldehyde. As a result of the abovementioned cross-linking, chitosan based hydrogels are generated [58].

Aldehyde based covalent cross-linking of chitosan results in a Schiff base reaction to form imine bonds [58, 60, 61]. Glutaraldehyde (GA) is a widely used covalent cross-linker of chitosan (Figure 1.15) due to its easy to produce synthetic feature and low cost [62]. However possible toxic nature of GA and its negative effect on the biocompatibility of chitosan limits its usage in especially biomedical areas [63]. Researchers have studied non-toxic, preferably natural cross-linking agents to replace GA [58, 62].

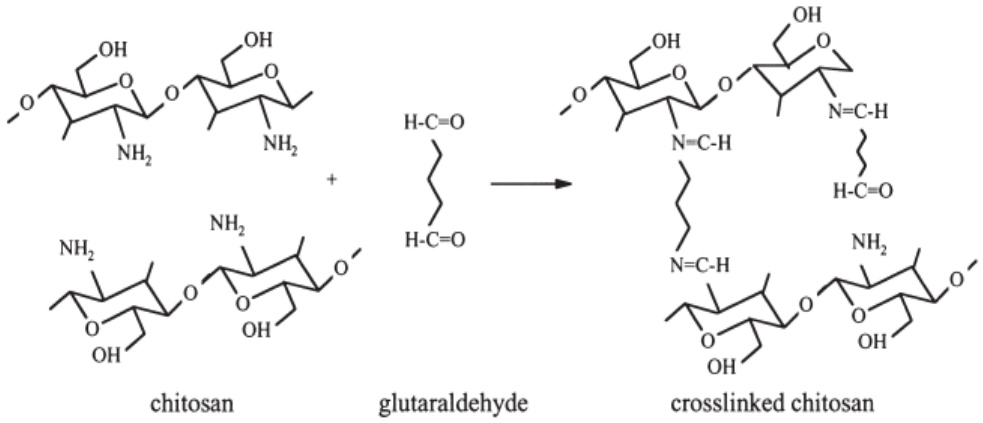

Figure 1.15 : Cross-linking of chitosan with glutaraldehyde. Adapted from Öztop, Saraydin [64]

Chitosan can be cross-linked ionically with any chemical compound that possesses at least two functional groups which generate a negative charge in water [65]. Ionic cross-linking of chitosan is generally provided by the formation of a physical network consisting of interactions between its positively charged -NH_2 groups and anionic molecules such as citrate, sulphate and sodium tripolyphosphate [66]. NaTPP

is a widely used ionic cross-linker of chitosan for producing hydrogels, beads or particles and its reaction mechanism is shown in Figure 1.16.

Ionic cross-linking is easily preferred over chemical cross-linking in some applications due to its ease of handling and does not include toxic cross-linker such as GA and genipin. However, covalently cross-linked chitosan is more stable in acidic solutions when compared to the ionically cross-linked version which can dissolve at a pH lower than 3.0 [65]. This situation limits the usage of ionically cross-linked chitosan in specific applications.

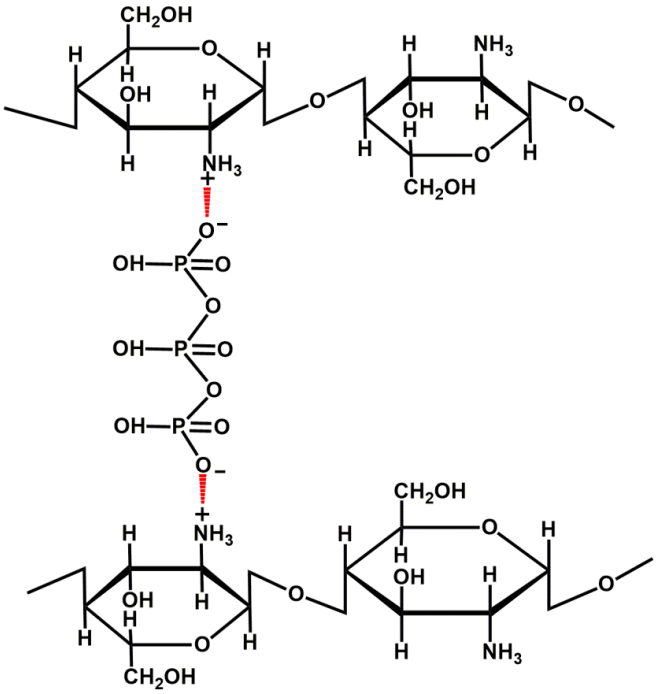

Figure 1.16 : Cross-linking of chitosan with NaTPP.

Apart from the cross-linkers mentioned above, researchers have been working on Schiff base reactions of chitosan with modified natural polymers in recent years due to their non-toxic and functional properties. As briefly mentioned above, the Schiff base is mainly about forming imine bonds thanks to a nucleophilic attack of amine to aldehyde groups as represented in Figure 1.17.

Formed imine bonds as a result of this interaction act as dynamic covalent bonds which provide self-healing property to the system [67]. Aromatic Schiff base linkages are more favorable than aliphatic ones due to their contribution to improving mechanical strength of generated hydrogel [68].

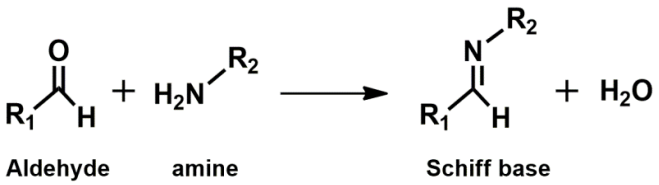

Figure 1.17 : Representation of aldehyde and amine interaction.

Many natural polymers have been modified by adding an aldehyde group to their polymer backbone to generate non-toxic and safe cross-linker alternatives for chitosan. Natural polymers such as alginate, pectin, guar gum, and xanthan gum have been the subject of these modifications [69-72].

In this thesis, xanthan gum is selected to be a subject of dialdehyde modification by oxidation to generate a non-toxic, safe and biocompatible cross-linker for chitosan.

1.2.2 Xanthan gum

Xanthan gum (XG) is anionic natural polymer that produced from a gram negative bacteria called Xanthomonas campestris via enzymatic biosynthesis. It can be classified as microbial polysaccharide due to its resource.

Structure of xanthan gum includes D-glucose, D-mannose, and D-glucuronic acid in a molar ratio of 2:2:1. Pyruvate and acetate are bound to D-mannose (Figure 1.18), depending on the production strain of bacteria and condition of culture [73].

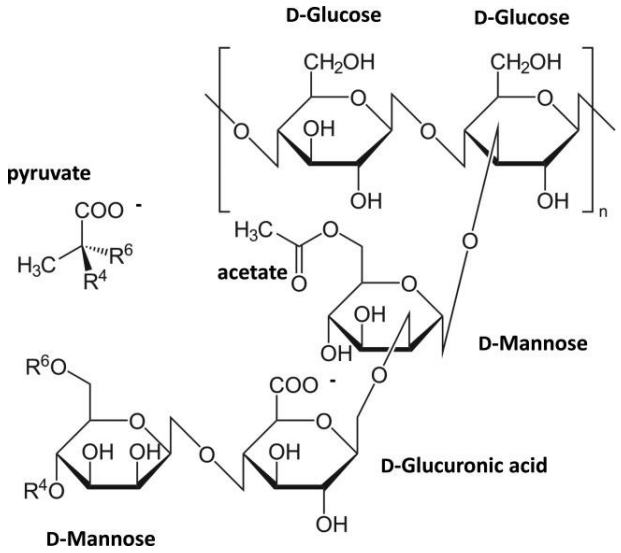

Figure 1.18 : Chemical structure of xanthan gum. Adapted from Petri [74].

Important features of xanthan gum are non-toxicity, biocompatibility, remarkable viscosity and swelling properties [75]. Thanks to its features, xanthan gum was

approved by the United States Food and Drug Administration (FDA) as a food additive and it can be used as an emulsifier, thickener and stabilizer. Apart from the food industry, xanthan gum is frequently utilized in medicine, agriculture, cosmetic and biomedical applications [75, 76].

The pyruvyl amount of xanthan gum in its structure determines the viscosity of xanthan gum in an aqueous solution. Lower pyruvyl indicates lower viscosity of gel due to creating less interaction between large molecules. However, the lower acetyl content of xanthan gum increases its gelling nature in an aqueous medium. Glucuronic acid and pyruvic acid make xanthan gum an anionic polymer [76].

Xanthan gum is not able to digest in the body easily. This feature of xanthan gum makes it a good candidate for food additive and drug delivery applications due to improving the passage of foods and drugs through the gastrointestinal tract [75, 76].

Thanks to its functional groups, xanthan gum can be physically and chemically cross-linked to form hydrogels, beads, particles. Physically cross-linking of xanthan gum requires various interactions such as electrostatic(ionic), hydrogen bonding and hydrophobic interactions [75].

IPN versions of xanthan gum are also widely studied to bring xanthan gum hydrogels to improved swelling and mechanical properties. The anionic nature of xanthan gum also allows it to physically interact with cationic polysaccharide chitosan. As a result of this electrostatic interaction, xanthan gum-chitosan PEC hydrogel can be formed [77].

1.2.3 Dialdehyde xanthan gum

In this thesis, dialdehyde xanthan gum (DXG) was synthesized to create a natural cross-linker alternative for chemical covalent cross-linkers of chitosan which can exhibit cytotoxic effects in clinic applications.

Anionic biopolymer xanthan gum is selected for this modification due to its properties which fulfil the requirements for drug delivery applications such as non-toxicity, biocompatibility, remarkable viscosity and high swelling capacity.

Sodium periodate oxidation is a commonly known procedure which is used in dialdehyde modification of gums. This modification involves converting

glucopyranose units of xanthan gum to aldehyde and creating extra functional sites for covalent cross-linking [78].

The oxidation procedure of xanthan gum is based on creating C-C cleavage between C2-C3 glucosidic bonds by oxidizing hydroxy groups in them in the presence of sodium periodate ($NaIO_4$). This generated cleavage then led to the formation of two aldehyde groups in each oxidized monomeric unit [78, 79]. As a result of the reaction dialdehyde xanthan gum is obtained.

Obtained oxidized xanthan gum, in another term, dialdehyde xanthan gum (DXG) can form Schiff base imine bonds by reacting with amino groups of chitosan as represented in Figure 1.19. Dynamic covalent cross-linking is provided by Schiff base reaction and can be used to prepare biocompatible, non-toxic chitosan-dialdehyde xanthan gum PECs, beads, microparticles [71, 79].

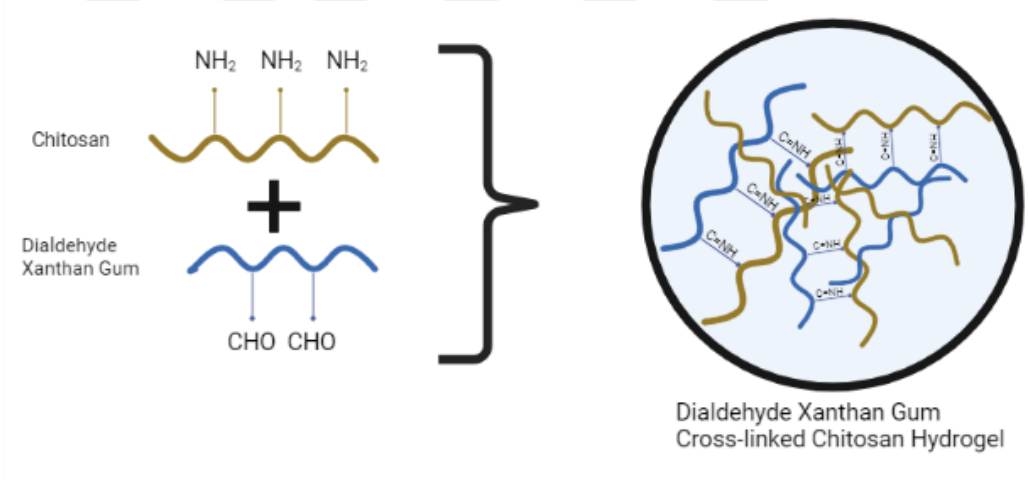

Figure 1.19 : Schematic representation of DXG-CH interactions.

1.2.4 *Trans*-cinnamaldehyde

In this thesis, *trans*-cinnamaldehyde (TC), with molar mass of 132,16 g/mol, is selected as an active molecule to be entrapped in CH-XG and CH-DXG matrices due to its remarkable antimicrobial properties.

Drug delivery systems developed for controlling human pathogens-related diseases (Figure 1.20), mostly employ conventional antibiotics as their active substances. However, studies of the last ten years indicate that human pathogens are gaining resistance to well known and widely employed antibiotics [80]. In order to deal with multi-drug resistant bacterial strains, researchers are working on natural active

molecules. Natural active molecules are showing high antibacterial efficiency with no stimulation of bacterial resistance.

FDA is identified TC as Generally Recognized as Safe (GRAS) material [81]. It can be considered as poorly water soluble terpene alcohol [82].

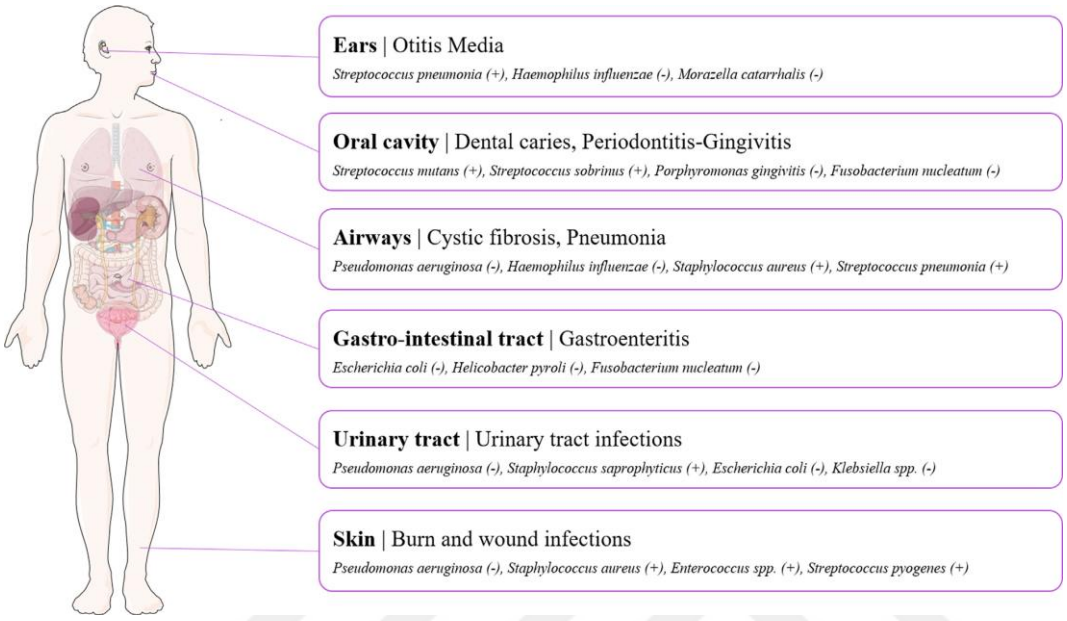

Figure 1.20 : Representation of pathogen related diseases in human body. Adapted from Birk, Boisen [80]

TC is one of the main ingredients of *Cinnamomum cassia* which exhibits antimicrobial, antioxidant, and antifungal properties [83, 84]. Antibacterial properties of TC have been studied and determined against numerous Gram-positive and -negative bacteria, such as E. coli, B. subtilis, Staphylococcus spp., Listeria spp. and Salmonella spp., Lactobacillus sakei, Vibrio spp., Pseudomonas spp., Porphyromonas gingivalis, Streptococcus pyogenes, and Cronobacter sakazakii [85].

Similar to most of the essential oils used in drug delivery systems, TC has to be encapsulated within water soluble polymers in order to increase its solubility in an aqueous medium.

Water soluble polymer xanthan gum can interact with TC via hydrogen and Van der Waals interactions due to functional groups in TC structure Figure 1.21. The Aldehyde group of TC can also interact with the amino group of chitosan which is one of the biopolymers used in this thesis.

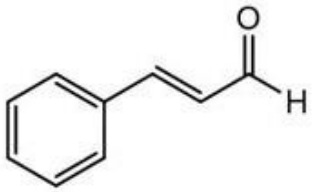

Figure 1.21 : *Trans*-cinnamaldehyde structure. Adapted from Do, Kim [86].

Like many phytochemicals, TC is also very vulnerable to losing its activity via degradation and volatilization. Encapsulation of TC provides this active molecule protection against enzymatic and pH-related degradations and also enhances its chemical stability [87].

1.3 Objective of Thesis

The aim of this study is to develop a biopolymeric matrice based non-toxic drug carrier via using modified xanthan gum and chitosan for the safe delivery of antimicrobial *trans*-cinnamaldehyde to gastrointestinal tract. This goal was achieved by the implementation of the following objectives:

- Production of natural polymer based cross-linker by sodium periodate oxidation of xanthan gum called dialdehyde xanthan gum
- Optimization of the synthesis method of *trans*-cinnamaldehyde loaded dialdehyde xanthan gum-chitosan microparticles
- Characterization of synthesized microparticles
- Determination of release behaviour of loaded microparticles in simulated conditions of the gastrointestinal tract

1.4 Hypothesis

Chitosan is a versatile biopolymer and is widely used in the encapsulation of conventional drugs and natural active molecules. Chitosan is dissolved in an acidic medium. This feature of chitosan makes chitosan pH-responsive in many drug delivery applications. However, in some targetted delivery operations, dissolution of chitosan in an acidic medium creates undesirable effects and interrupts reaching its encapsulated active molecules to predestinated release environment.

The dissolution behaviour of chitosan in an acidic environment is highly related to its amine groups. Covalent cross-linking of chitosan through its amine groups can reduce its acidic solubility. However, most of the commercially available covalent cross-linkers of chitosan are synthetic and exhibit toxic effects.

Xanthan gum is an anionic natural polymer that can interact with cationic chitosan to form a polyelectrolyte complex (PEC) which is a suitable structure for entrapping active molecules or drugs. Most of the driving force of this PEC formation is based on weak electrostatic interactions.

In this study, a natural polymer with the covalent cross-linker ability for chitosan was synthesized and it was used to create more stable polymeric matrice based microparticles by using these two polymers. *Trans*-cinnamaldehyde loaded biopolymeric matrice based microparticles enable the delivery of its active molecules through the gastrointestinal tract that exhibits acidic and slightly basic pHs at different sections.

Covalent crosslinking of chitosan with dialdehyde xanthan gum improves the physicochemical properties of chitosan and provides reduced solubility in acidic environments.

The hypothesis of this study is that microparticles created by covalently cross-linking of chitosan with dialdehyde xanthan gum can route its antimicrobial active molecules to the intestinal region of the body without losing it via undesired release in acidic gastric conditions. The offered system can be a safe and non-toxic alternative for drug delivery application to the gastrointestinal tract in the near future.

2. MATERIALS AND METHODS

2.1 Materials

Chitosan (LMW) with the deacetylation degree of 76%, Sodium Hydroxide (NaOH), Acetic Acid, Hydrochloric Acid (HCl), Sulphuric Acid (H_2SO_4), Sodium Tripolyphosphate (NaTPP), Sodium periodate ($NaIO_4$), and Ethanol (99,8%) were obtained from Sigma-Aldrich. Xanthan gum (≥99,9 purity) was purchased from Ataman Chemichals. *Trans*-cinnamaldehyde was provided by Salus Nutra Inc. Phenolphitalein solution (1%) was purchased from Labchembio. Ethylene glycol, Tween 80 and Sodium bicarbonate ($NaHCO_3$) were purchased from Merck. Phosphate Buffered Saline (PBS) tablets was purchased from MP Biomedicals.

2.2 Synthesis and Characterization of Dialdehyde Xanthan Gum

In order to obtain dialdehyde xanthan gum (DXG), xanthan gum was modified via sodium periodate oxidation which is previously described in literature [71, 79]. Sodium periodate oxidation of xanthan gum (XG) is schematically represented in Figure 2.1.

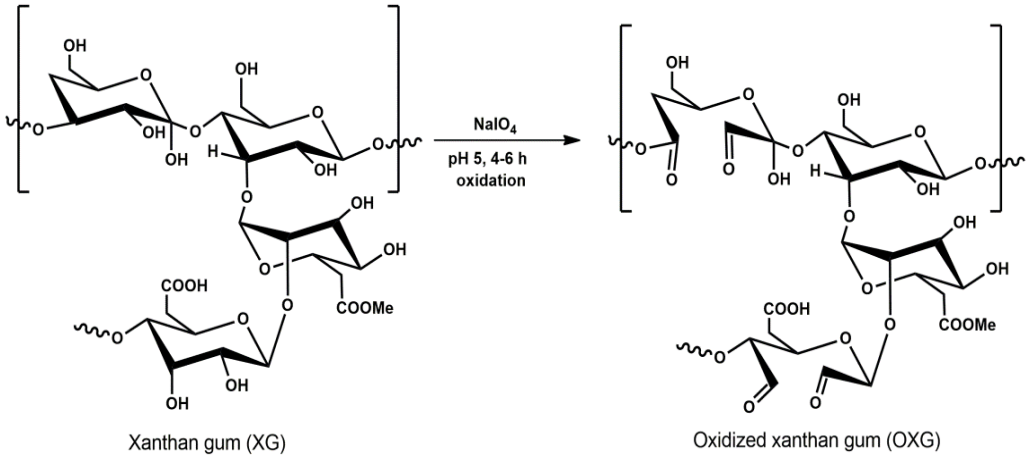

Figure 2.1 : Dialdehyde xanthan gum synthesis. Adapted from Ngwabebhoh, Zandraa [79].

Briefly, 200 ml of XG solution was prepared by dissolving 2 grams of XG in distilled water at 60 ^{o}C. After complete dissolution of XG, the temperature of solution was allowed to cool down to 40 ^{o}C. Then, 20 ml of 0.096 g/ml $NaIO_4$ solution was poured into XG solution under magnetic stirring. After that pH of mixture was adjusted to pH 5.0 by using 2.0 M H_2SO_4 and kept constant under continuous stirring in dark environment for at least 4-6 hours.

Reaction was ended by adding 1 ml ethylene glycole into the mixture or pouring mixture into equivalent volume of ethanol for different versions of synthesis. After reaction was ended, oxidized XG mixture was loaded into dyalysis bag with 12 kDa cut-off and dialysed for 5 days for each version of synthesis. After dialysis, purified sample was lyophilized for 4 days to obtain dried DXG.

2.2.1 Determination of oxizidation degree of XG

The oxidization degree of XG was determined via the titration method based on quantitative alkali consumption which is described in the literature [88].

Briefly, 10 ml of 0.2 M NaOH stock was prepared and poured into a flat bottom flask. Then 0.2 grams of DXG was added into the flask. The obtained mixture was magnetically stirred at 70 ^{o}C for approximately 4 minutes to obtain complete dissolution of DXG. After that, the flask was cool down quickly under tap water. 10 ml of 0.2 M H_2SO_4 and 50 ml of distilled water were added to cooled down the temperature of the mixture respectively under stirring.

As a final step, 200 µl of 0.2 % phenolphthalein was added and the solution was titrated against 0.2 M NaOH to obtain a stable pink color which is a sign of the ending of the titration. The same titration procedure was also followed for XG as a control. The percentage of dialdehyde groups of DXG was calculated with the equation 2.1 below:

$$CHO\% = \frac{(V_{oxidized} - V_{control}) \times (C_{NaOH})}{8 \times \frac{m}{MM}} \qquad (2.1)$$

Where $V_{oxidized}$ and $V_{control}$ refer to volumes of NaOH which are used to reach the endpoint of the titration of DXG and XG repectively. C_{NaOH} is the molar concentration of NaOH which is used during titration and m is the weight of XG in

gram. MM is the molar mass of the repeating unit of XG used in this study which is 934 g/mol.

2.2.2 Fourier transform infrared spectroscopy (FTIR) analysis

FTIR measurements were carried out by using Jasco FTIR 4700 device in order to confirm aldehyde groups on dried samples of DXG and identify functional groups of compounds.

2.3 Encapsulation of *Trans*-cinnamaldehyde

Encapsulation of *trans*-cinnamaldehyde was carried out by following two strategies. The first strategy, which forms the basis of this thesis, is based on creating a biopolymer matrice with DXG and CH. The process was optimized with different DXG, CH and TC concentrations.

Briefly, 0.7 % CH was dissolved in 25 ml of acetic acid solution (0.5 %) for the duration overnight, then its pH was adjusted to 5.5 with 1 M NaOH solution. DXG was dissolved in 25 ml of distilled water for the duration overnight and its pH was adjusted to pH 7.0. After that, 150 µl Tween 80 is added and dissolved in DXG solution to create an emulsifying effect for TC, then 160 µl of TC is added to the DXG solution under continuous stirring. DXG-TC mixture was homogenized with Bandelin Sonopuls HD 4200 ultrasonicator with T213 probe at 50 % amplitude for 1 minute in an ice bath to control overheating.

After the homogenization step, the solution was loaded into a sterile syringe and then was added into chitosan solution drop by drop under stirring. The final mixture was ultrasonicated at 50 % amplitude for 3 minutes in an ice bath to control overheating and left on a magnetic stirrer at 500 rpm for 24 hours. Before the experiment was ended, the pH of the suspension was adjusted to pH 8.0 using 0.2 M NaOH to obtain more stable (less reversible) imine bonds [79].

In order to collect the synthesized particles, the suspension was loaded into 50 ml falcons and centrifuged at 9000 rpm for 30 minutes. After centrifugation, supernatants were removed and saved for encapsulation efficiency analysis while pellets were lyophilized for 5 days to obtain dried particles.

The same procedure was followed step by step for producing control groups of the above mentioned particles by replacing DXG with XG. As a result of the followed procedure, CH-XG microparticles were obtained with polyelectrolyte complexation and ionotropic gelation methods.

2.4 Characterization of Microparticles

2.4.1 Spectrometric analysis

UV-vis measurements were employed to determine unknown TC concentrations in supernatants obtained from encapsulation processes and in release buffers of microparticles.

TC was diluted with ethanol in quartz cuvette at known concentrations and then its absorbance was measured at 285 nm. Obtained data from the measurement were used for developing the calibration curve of TC.

On the other hand, FTIR was utilized to determine surface characterization of developed microparticles. Obtained data from FTIR analysis were also used in verifying TC encapsulation in microparticles by examining characteristic absorption peaks of TC, CH-XH and CH-DXG samples.

2.4.2 Encapsulation efficiency and loading capacity determination

The calibration curve of TC was developed for TC between 0.5 μg/ml and 5 μg/ml. Then it was used to determine the non-encapsulated TC amount.

Briefly, supernatants of microcapsules were filtrated with a 0.2 μm Whatman filter then filtrated supernatants of each version of microparticles were diluted with ethanol in a quartz cuvette and absorbance at 285 nm was measured. Concentrations of non-encapsulated TC in supernatants were determined by using the calibration curve of TC.

Encapsulation efficiency of produced microparticles was determined according to equation 2.2 below:

$$EE\% = \frac{Total\ amount\ of\ TC\ added - Free\ TC\ amount}{Total\ amount\ of\ TC\ added} \times 100 \qquad (2.2)$$

In order to determine the loading capacity of microparticles, dry weight of microparticles was measured and put into the equation 2.3 below:

$$LC\% = \frac{Total\ amount\ of\ TC - Free\ TC\ amount\ in\ supernatant}{Total\ weight\ of\ microparticles} \times 100 \qquad (2.3)$$

2.4.3 Particle size and zeta potential analysis

Optimized versions of microparticles were subjected to dynamic light scattering (DLS) and zeta potential analysis in order to determine their size, size distribution and surface charge.

Liquid samples, which were taken from suspensions of microparticles before the lyophilization process, were analyzed by using Malvern Zetasizer Nano ZS with the configuration of 173^{o} backscatter and 1.330 refractive index at 25^{o}C. Briefly, samples were diluted with distilled water in disposable polystyrene cuvette, then the cuvette was placed into the device for particle size analysis. Analysis was performed with 3 cycles with 15 rounds for each sample.

The surface charge of microparticles which affects their electrophoretic mobility was determined by Zeta potential analysis. Analysis was performed with the same device by using disposable zeta cuvettes. The same procedure and configurations were also applied for zeta potential analysis.

2.4.4 Differential scanning calorimetry analysis

Differential scanning calorimetry (DSC) is a thermo-analytic method which can be used to describe the thermal profile, possible fusion and crystallization behaviour of microparticles. TC encapsulation within the produced microparticles can also be confirmed with a comparison of the thermal profile of particles and their control groups.

DSC analysis of TC, XG, DXG, CH and microparticles was performed with Shimadzu DSC-60 instrument. In brief, 1 mg of each sample was placed into aluminum cells and analyses were performed in the temperature range between 25 ^{o}C and 300 ^{o}C. The temperature range was selected based on literature that suggests possible endothermic and exothermic peaks could be found in this range [71, 89].

2.4.5 Surface morphology analysis

The surface morphology of produced microparticles was determined by scanning electron microscopy (SEM). TC loaded CH-DXG microparticles and their control groups were subjected to SEM analysis to gain information about their shape, texture and porosity which can affect their release behaviour and mechanical strength. Lyophilized microparticles were coated with a conductive material and then scanned at 10kV in different magnifications.

2.4.6 Determination of in-vitro release behaviours

In-vitro release studies of TC from microparticles were conducted in simulated gastrointestinal tract conditions as previously described in the literature [79]. Two different 10 mM of PBS buffer stock solutions were prepared and their pH values were adjusted to pH 2.0 and 7.0. The release behaviour of microparticles in the gastric fluid was simulated by PBS buffer with pH 2.0 while intestinal fluid was simulated by PBS buffer with pH 7.0.

25 mg of microparticles were weighed and added into 25 ml of PBS buffer at pH 2.0 and pH 7.0. Then, suspensions were placed on an orbital shaker performing at 100 rpm and 37^{o}C . For each buffer, 1 ml of sample was collected from release mediums and an equivalent volume of fresh PBS was added into the release medium hourly during first 8 hours, then 24th and 96th hours.

Obtained samples were centrifuged and their supernatants were analyzed with UV-vis measurements at 285nm. The amount of released TC was determined by using collected absorbance data from analysis with the help of a previously developed TC calibration curve. Then, the cumulative release of TC was calculated with the equation 2.4 below:

$$Cumulative\ Release\ \% = \frac{Released\ amount\ of\ TC}{Loaded\ amount\ of\ TC} \times 100 \qquad (2.4)$$

3. RESULTS AND DISCUSSION

3.1 Optimized Dialdehyde Xanthan Gum

During the optimization of the synthesis processes of DXG, three versions were synthesized. Versions were differentiated from each other in terms of reaction time and agents which are used to stop the reaction. The selected version to be used in the further experiment in this thesis was determined by comparing their oxidization degree which indicates the dialdehyde percentage of synthesized DXG. According to the titration method based on quantitative alkali consumption, oxidization degrees of created versions were calculated by using equation 2.1 and the results were shown in Table 3.1 below:

Table 3.1 : Optimization parameters of synthesized DXG versions

Versions	Reaction Time	Ending Agent	Degree of Oxidization %
DXG1	4.7 h	Ethylene Glycol	29.4
DXG2	5.8 h	Ethanol	16.4
DXG3	24 h	Ethylene Glycol	10.5

After reactions were ended, every version of DXG was loaded into the dialysis membrane, then dialyzed for 5 days in distilled water at pH 7.0. During dialysis process, dialysis water was renewed twice a day. After dialysis was ended, collected samples were frozen and then lyophilized for 4 days for each version (Figure 3.1).

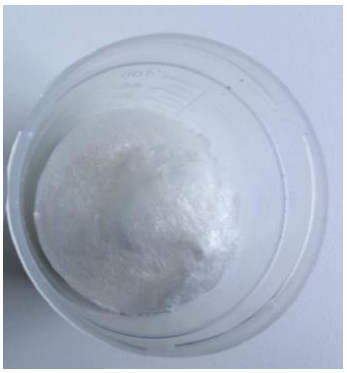

Figure 3.1 : Appearance of DXG1 after lyophilization

Best oxidization degree was obtained in the case of DXG1 which consumed 11.865 ml of 0.2 M NaOH to reach the stable pink colour, indicating end point of titration while XG, as a control group, consumed 9.450 ml of 0.2 M NaOH. Conversion of color shade into stable pink color during titration of DXG1 is represented in Figure 3.2.

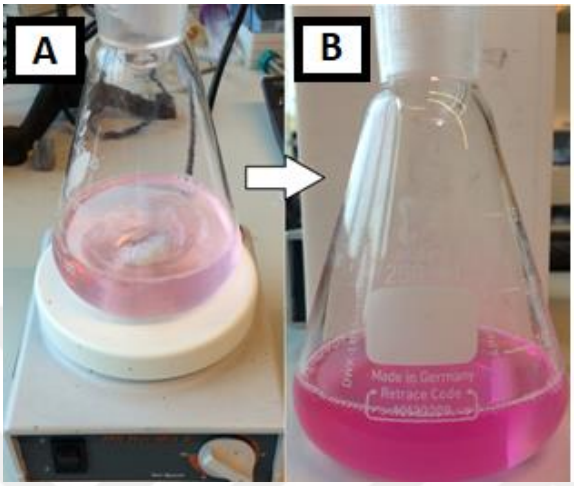

Figure 3.2 : Stable pink color formation during alkali titration of DXG1; instant pink color appearance (A), stable pink color appearance at the end of titration (B)

Another interesting note from optimization processes is that the amount of obtained DXG3, which was approximately 0.5 g after the drying process, was quite low. The theoretical dry weight of each version after the lyophilization process is to be expected around 2.0-2.5 g. This low amount of DXG3 might be due to its long reaction time of about 24 hours which shortens its polymer chains too much and cause polymer loss during dialysis.

It was observed that ethylene glycol was more suitable agent for stopping reaction in terms of its low usage amount and easy elimination of its residue from the system during dialysis. On the other hand, ethanol was found to be more problematic because it was hard to eliminate completely during dialysis due to its high amount of usage during stopping the reaction.

DXG1 was chosen to be used in further experiments due to its dialdehyde content of 29.4 % which is quite similar to previous studies found in the literature [79]. In order to confirm aldehyde groups presented in DXG1, FTIR measurement was applied. Theoretically, it was expected to observe bands due to C=O stretching provided by aldehyde groups at wavenumbers between 1650-1750 cm^{-1}. However, xanthan gum

has C=O stretching around at 1700 cm^{-1} due to having acetate groups [90]. FTIR spectra recorded for XG and DXG1 were shown in Figure 3.3.

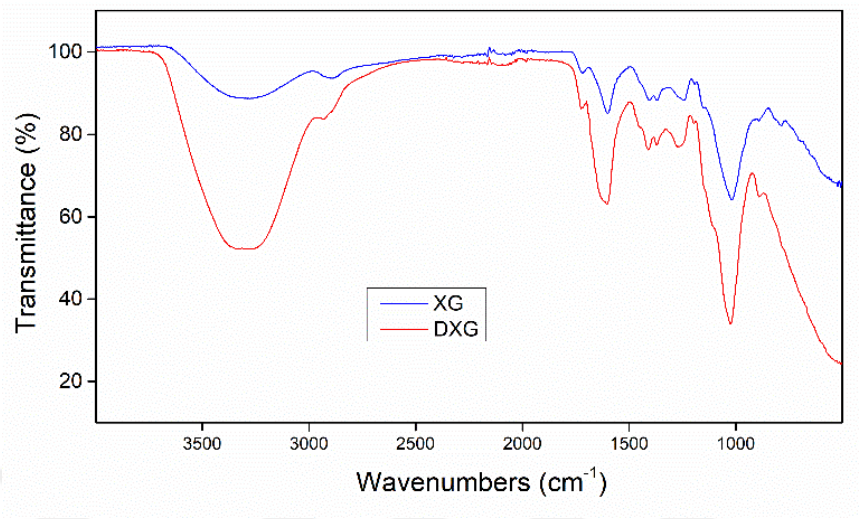

Figure 3.3 : FTIR spectra of XG and DXG1

As can be seen in Figure 3.3, the occurrence of a strong peak at 3200 cm^{-1} might be due to the -OH stretching vibration of repeated pentasaccharide units of both XG and DXG. Absorption bands around 1612 and 1408 cm^{-1} were assigned to asymmetric and symmetric stretching peaks of the carboxylate groups of glucuronic acid units of both XG and DXG. On the other hand, the peak at 1730 cm^{-1} that was seen in the XG spectrum shifted to 1722 cm^{-1} in the DXG spectrum, which might indicate C=O stretching vibration from the introduced aldehyde groups of DXG. The peaks observed at 1244 and 1017 cm^{-1} for XG were also shifted to 1271 and 1028 cm^{-1} for DXG, belonging to C-O and C-O-C stretching vibrations, respectively.

These results were similar to previous studies [71, 91]. It was concluded that the spectral shifts observed upon a comparison of FTIR spectra of both XG and DXG confirmed the modification of xanthan gum with sodium periodate oxidation.

3.1.1 Characterization of microparticles

3.1.1.1 Optimization of microparticles

In order to examine physical interactions and cross-linking effects on the created delivery system, the experimental setup was kept wide. Synthesis of TC loaded CH-DXG and CH-XG microparticles were performed with their control groups.

In order to determine the effect of ionic cross-linking in the system, non-toxic cross-linker NaTPP was selected to interact with amine groups of chitosan. Thanks to control groups which are produced via polyelectrolyte complexation (PEC) and ionotropic gelation (IG) methods, the effect of covalent cross-linking provided by DXG to the biopolymeric matrice will be comprehensively examined. Synthesized groups were named under two notations; IC notation represents 'ionic complex' and CC notation represents 'covalent cross-linking'. The experimental setup is shown in Table 3.2 below:

Table 3.2 : Experimental setup

Name	Assembly Compounds
IC-1	CH + XG
IC-2	CH + XG + NaTPP
IC-3	CH + XG + TC
IC-4	CH + XG + NaTPP + TC
CC-1	CH + DXG
CC-2	CH + DXG + NaTPP
CC-3	CH + DXG + TC
CC-4	CH + DXG + NaTPP + TC

IC group was produced according to Argin-Soysal, Kofinas [89] study with modifications. Preliminary production of groups consists XG was performed using 0.7 % CH at pH 5.5 and 0.7 % XG at pH 7.0. Chitosan solution's pH was critical to maximize ionic interaction between protonated amine groups of CH and carboxyl group of XG.

Concentrations and pH values of the solutions can directly affect cross-linking densities and swelling behaviours of the capsules. Concentration of 0.7 % was selected for each polymer for the experiment because CH and XG complexes showed optimized swelling behaviour at this concentration.

Production process of first version (v1) of empty IC-1v1 particles, was involved adding 50 ml of 0.7 % XG solution drop by drop into 50 ml 0.7 % of CH solution under stirring at 500 rpm. The formation of beads was observed due to CH-XG complexation. Then the particle suspension was sonicated at 50 % amplitude for 3 minutes in an ice bath and then stirred for 45 minutes. However, it was observed that

applied homogenization process in order to control the size of the beads had an impact on the shape of the beads (Figure 3.4).

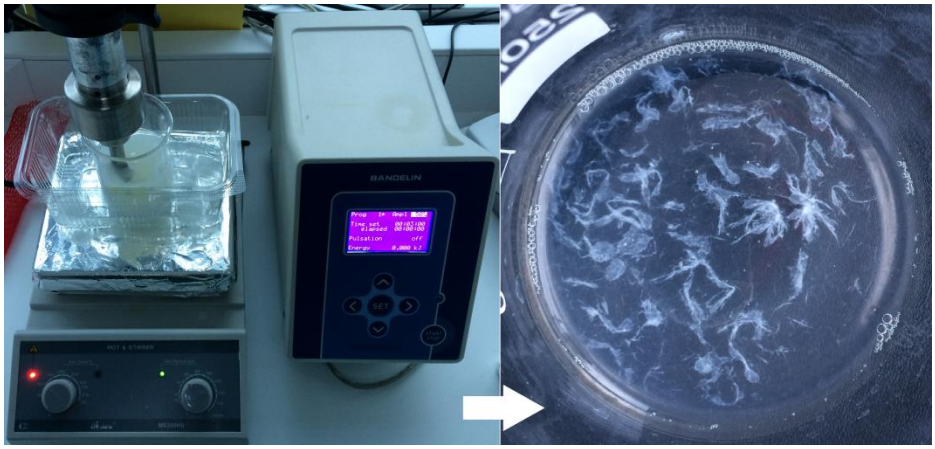

Figure 3.4 : CH-XG particles after homogenization process

IC-2v1 particles were produced by following the abovementioned procedure except for the addition of 25 ml of 0.2 % NaTPP (pH 3.7) into the mixture drop by drop after bead formation. Then, the final solution was sonicated for 3 minutes and then stirred at the same configurations. Unlike IC-1v1, no clumsy structure was observed after the homogenization process. This might be due to the cross-linking effect provided by NaTPP and it indicates ionotropic gelation helped to improve the mechanical strength of the CH-XG complex.

TC loaded IC-3v1 and IC-4v1 particles were produced by following the previously mentioned IC-1v1 and IC-2v1 procedures respectively. However, 350 µl of TC was added into their XG solutions with 350 µl of Tween 80 and the mixture was emulsified by ultrasonication for 30 seconds at 50 % amplitude. Then, the rest of the procedures were applied to each system respectively.

While production of IC-3v1, it was observed that beads were formed before sonication, then corrupted and disappeared after sonication. The final solution was emulsified which can be due to corruption of pre-generated CH-XG beads allowing TC to mix with chitosan solution. However, IC-4v1 has shown a less dramatic effect in terms of corruption of beads due to NaTPP cross-linking compared to IC-3v1.

After production of all versions, suspensions of coacervates were centrifuged at 9000 rpm for 30 minutes. Supernatants were removed and collected for further analysis. Pellets were frozen and then lyophilized to obtain dried particles.

Based on the information collected during the production of the IC group, the same way CC group was produced. DXG1 was employed during the production of this group. Production procedures for CC-1v1 and CC-2v1 formulations were exactly the same as IC versions except XG was replaced with DXG at the same concentration.

CC-3v1 was produced by adding 50 ml of 0.7 % DXG solution drop by drop into 50 ml of 0.7 % CH solution under stirring at 500 rpm. Unlike bead formation observed in IC-3v1, shapeless gel clumps were observed. Then the suspension was sonicated at 50 % amplitude for 3 minutes in an ice bath. By the effect of the sonication process, gel clumps were corrupted and then disappeared. However, during the magnetic agitation of the formulation, new gel clumps were formed and disappeared simultaneously.

This may be the result of the aldehyde content of DXG1 that interacts with amine groups of CH by Schiff base reaction and forms self-healing imine bonds. After 45 minutes of stirring, the mixture was centrifuged. After centrifugation, there was no pellet observed. Interestingly during centrifugation, gel clumps interacted with each other and formed an intact hydrogel as shown in Figure 3.5.

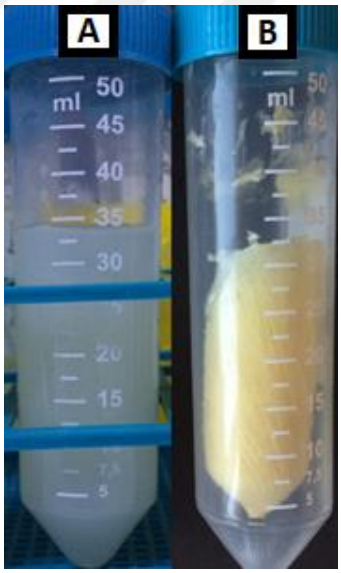

Figure 3.5 : CC-3v1 formulation after centrifugation (A), after lyophilization (B).

Intact hydrogel formation of CC-3v1 formulation might be related to G force since it has been exposed during centrifugation. Applied G force may induce the formation of imine bonds of the generated system and this situation might create an intact hydrogel which can hold all water content of the system.

On the other hand, the CC-4v1 formulation was not suffered from the formation of gel clumps and intact hydrogel formation during centrifuge. Its pellet and supernatant were collected after the centrifuge process. This might be due to NaTPP interaction with some of the amine groups of CH that is keeping them occupied against imine bond formation due to aldehyde groups of DXG. Theoretically in CC-4v1 formulation, there can be dual cross-linking of chitosan both ionically and covalently. Final appearances of first versions after lyophilization and their FTIR specta can be seen in Appendix A.

After data was collected from the first versions for each group, the production procedure was optimized for DXG versions in terms of reaction time and DXG concentrations. Imine bond can be considered a dynamic interaction and it requires more time to settle. Moreover, the employed concentration of DXG in the first versions can be considered to be quite high for synthesizing micron-sized particles according to experience from the previous experiment.

Experiments with small volumes were performed for the DXG group by using concentrations of DXG as 0.7, 0.3, 0.2, 0.15% and a long reaction time of 24 hours. For these experiments, the volume of the polymer solution was determined as 5 ml for each polymer and the concentration of chitosan was kept at 0.7 %.

According to observational data, DXG concentration of 0.7 % in 24 hours reaction without a homogenization process has resulted in particle formation in coacervates. However, it was observed that gel clumps appeared in the first hour of the agitation period of the CC-3 system. Then appeared gel clumps were degraded into relatively small particles during 24 hours of agitation process of the system which is shown in Figure 3.6.

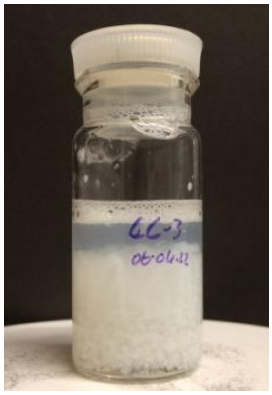

Figure 3.6 : Final appearance of CC-3 formulation synthesized with 0.7 % of DXG1.

In order to obtain smaller particles, same procedure was followed by using 0.3 % DXG. Final appearance of this group was shown in Figure 3.7.

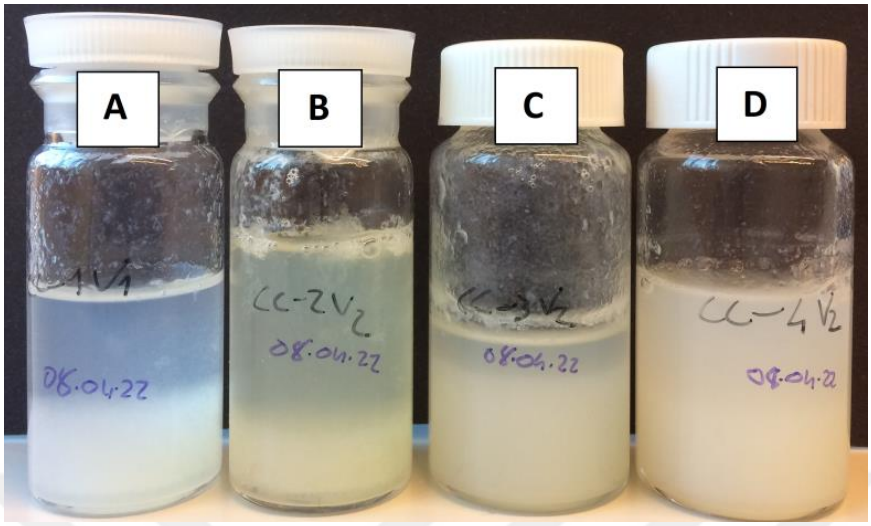

Figure 3.7 : Final appearance of DXG group produced with 0,3 % DXG1; CC-1 (A), CC-2 (B), CC-3 (C), CC-4 (D).

Although progress has been made in reducing particle size and avoiding bulk hydrogel formation, it has been observed that the resulting coacervates still consist of relatively large particles.

The amount of 0.2 % of DXG was tried to decrease particle size after abovementioned trial. However, gel formation could not be avoided during the first hour of agitation (Figure 3.8).

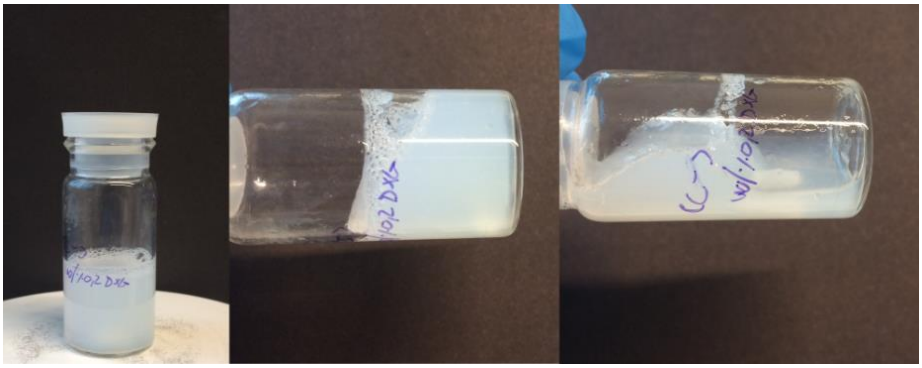

Figure 3.8 : Appearance of gel formation in CC-3 prepared with 0,2 % DXG1 after one hour of agitation.

This result indicates that the formation of gel is not highly dependent on DXG concentration. It might be related to the short reaction time which prevents polymer complex from reaching a stable state in terms of imine bond formation. It was also

electrostatic forces involved in this formation due to the anionic charge of xanthan gum. The long reaction of 24 hours can provide a more stable interaction within the polymers of the system. This suggestion was supported by no gel formation of CC-4 formulation which utilized NaTPP as an ionic cross-linker.

The final concentration of DXG, which was used in the further experiment of this thesis, was determined as 0.15 % according to the small volume preliminary experiment (Figure 3.9).

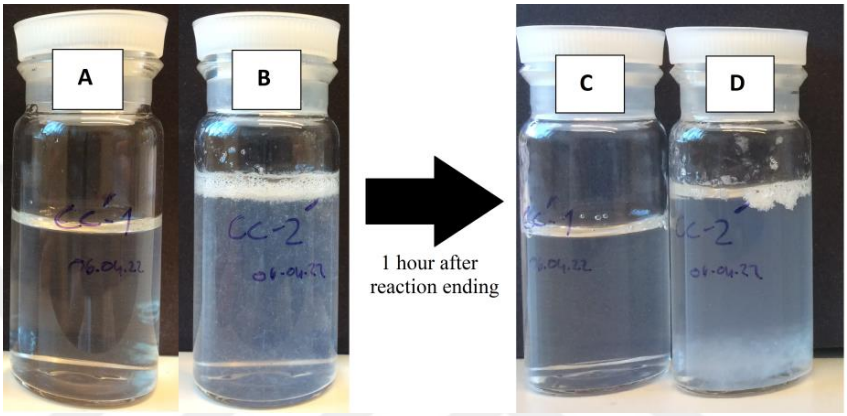

Figure 3.9 : Appearance of CC-1 and CC-2 produced with 0.15 % of DXG1 one hour later after reaction ending; CC-1 (A), CC-2 (B).

Optimized versions were synthesized using 0.15 % of DXG via following the steps describing in method section (Figure 3.10). To obtain control groups, IC group was prepared by using 0.15 % of XG.

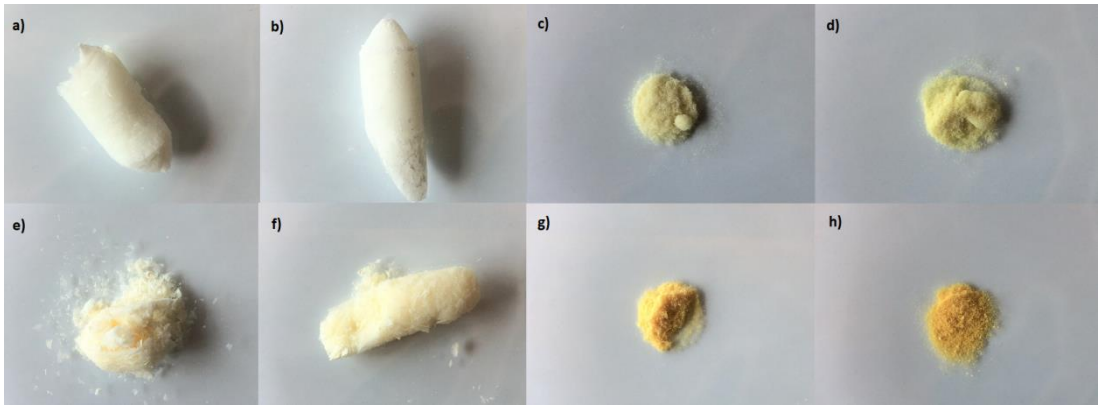

Figure 3.10 : Optimized versions of formulation after lyophilization; a) IC-1v2, b) IC-2v2, c) IC-3v2, d) IC-4v2, e) CC-1v2, f) CC-2v2, g) CC-3v2 h) CC-4v2

IC group exhibits lighter color for both empty and loaded versions after drying. Saturated color of CC group might be related to its aldehyde content.

3.1.1.2 Determination of encapsulation efficiency and loading capacity

Encapsulation efficiencies of TC loaded microparticles were evaluated by analyzing their supernatants with an UV spectrophotometer at 285 nm. Obtained absorbance values were processed to determine free TC concentration in supernatants via using the calibration curve of TC (Figure 3.11).

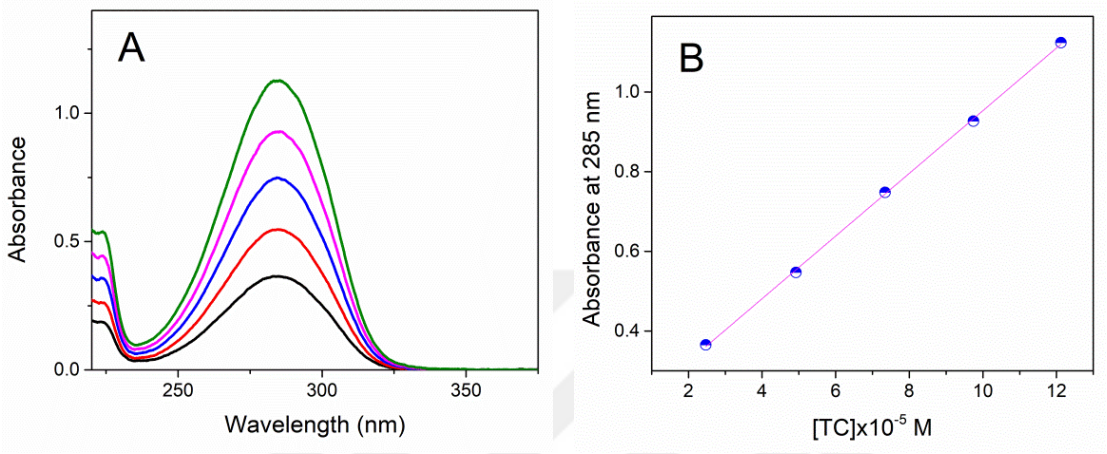

Figure 3.11 : A) UV-vis spectra of TC depending on concentration. B) Absorbance values at 285 nm upon various concentration of TC.

According to equation 2.2 and 2.3, encapsulation efficiencies and loading capacities of final version (v2) of optimized particles were determined and listed in the Table 3.3. Detailed information about encapsulation efficiencies and loading capacities of all synthesized versions can be seen in Appendix A at Table A.1.

Table 3.3 : Encapsulation efficiencies and loading capacities of loaded particles

Versions	Encapsulation Efficiency (%)	Loading Capacity (%)
IC-3v2	87.94	44.95
IC-4v2	79.49	45.91
CC-3v2	80.06	43.57
CC-4v2	68.88	43.05

It was observed that the loading capacities of synthesized particles were quite close. However, CC-4v2 has shown the lowest efficiency for encapsulation. Process conditions were kept identical for all versions. The encapsulation efficiency of IC-4v2, which was produced as a control group of CC-4v2, also showed the lowest encapsulation efficiency in its experimental group.

This situation might be caused by cross-linking with NaTPP has a negative effect on formation of polymer complex. On the other hand, IC-3v2 and CC-3v2 formulations, which might tend to form a more complex network, can entrap more TC in their networks.

3.1.1.3 Particle size and zeta potential analysis

DLS measurements have been performed for both empty and loaded particles to observe whether TC loading has any effect on particle size. Empty particles for both final versions of optimized experiment groups, which are IC-1v2 and CC-1v2, have shown significant difference in terms of particle sizes and distributions (Figure 3.12(A)).

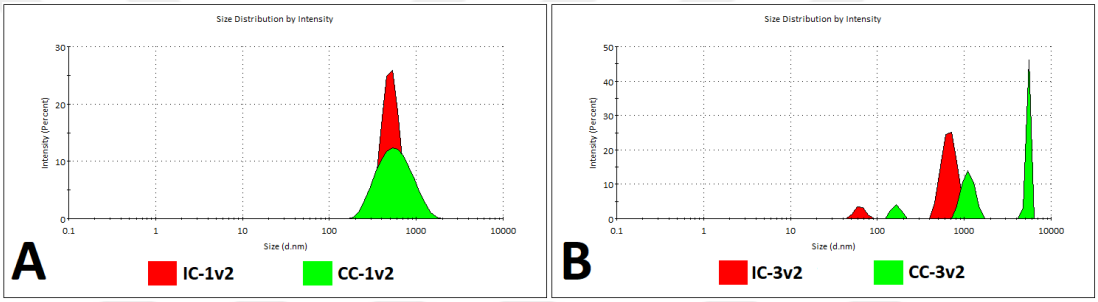

Figure 3.12 : Size distribution of synthesized particles; empty IC-1v2 and CC-1v2 particles (A), TC loaded IC-3v2 and CC-3v2 particles (B)

According to DLS measurements, IC-1v2 empty particles have an average diameter of 647.4 nm with 0.542 polydispersity index (PDI). On the other hand, CC-1v2 empty particles have an average diameter of 466.9 nm with 0.244 PDI value. These results revealed that the particle size distribution of CC-1v2 is more homogenous compared to IC-1v2. Covalent cross-linking of CC-1v2 formulation might provide more stable particles to the system which can avoid agglomeration.

However, TC loaded IC-3v2 and CC-3v2 particles exhibited quite large average particle size distribution and PDI compared to their empty controls groups (Figure 3.1(B)).

As can be seen in Figure 3.12 (B), the size distribution of CC-3v2 was too wide and it consists of micron sized particles. CC-3v2 has an average diameter of 6.03 µm and particles with 0.310 PDI value. However, this measurement cannot be accepted as verifiable due to over micron size particles were estimated by an algorithm of the instrument. Malvern Zetasizer Nano ZS is an instrument that can measure particles

under 1.0 micron with high precision. On the other hand, IC-3v2 has 693.7 nm average diameter and particles with 0.519 PDI. The particle size difference between these two versions can be related to coalescence that CC-3v2 formulation may have suffered due to the late analysis of particles production which has to hold in a liquid state. Depending on above mentioned results besides instrumental error margin, we can say that TC loading has affected the size of microparticles as expected.

Zeta potential analysis has been performed to obtain data about the surface charge of microparticles. The average zeta potential of IC-3v2 and CC-3v2 were found to be 5.60 mV and 9.13 mV, respectively (Figure 3.13).

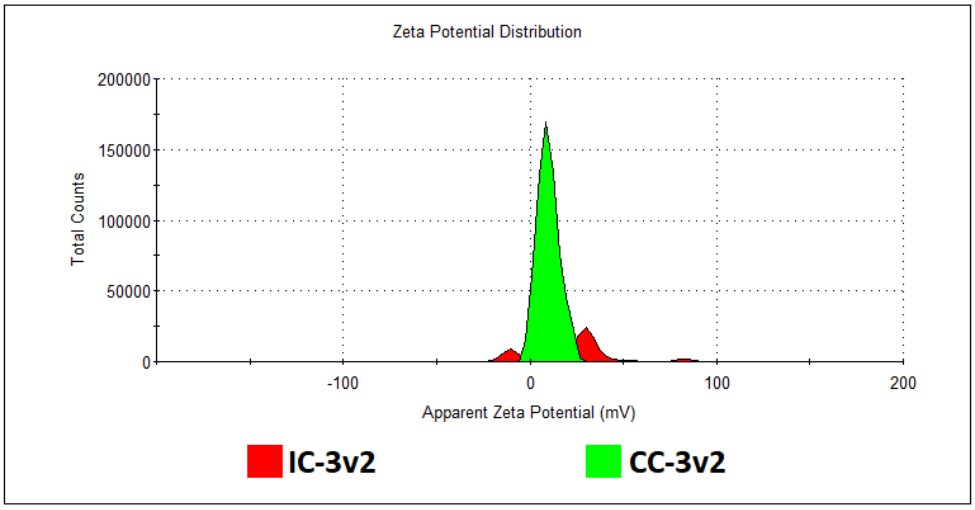

Figure 3.13 : Zeta potential distributions of IC-3v2 and CC-3v2

Zeta potentials of synthesized microparticles have to be positive due to the cationic charge of chitosan which was used in higher concentration compared to xanthan gum and dialdehyde xanthan gum. Amine groups of chitosan make this polymer cationic. However, microparticle formation is highly related to amine groups of chitosan which can negatively affect its positive zeta potential.

Microparticles were prepared by transferring XG and DXG solutions with TC into CH solution drop by drop. This situation has to make CH as a coating polymer of particles. However, the applied homogenization step may affect created structure and the anionic charge of xanthan gum can demonstrate itself in the system.

CC-3v2 was showed higher and more uniform zeta potential comparing to IC-3v2. This indicates a new homogenous structure of CC-3v2 and a non-uniform structure of IC-3v2 which can demonstrate features of its constituent polymers separately due

to free polymers left in the system. We can say that both two systems can tend to flocculate in suspension because their zeta potentials are in the range of +/- 25 mV [92].

3.1.1.4 FTIR analysis

FTIR analysis has been performed on synthesized microparticles and their assembly components to verify cross-linking of polymers and also to verify the loading of the active molecule to the system. FTIR spectrum of TC is shown in Figure 3.14.

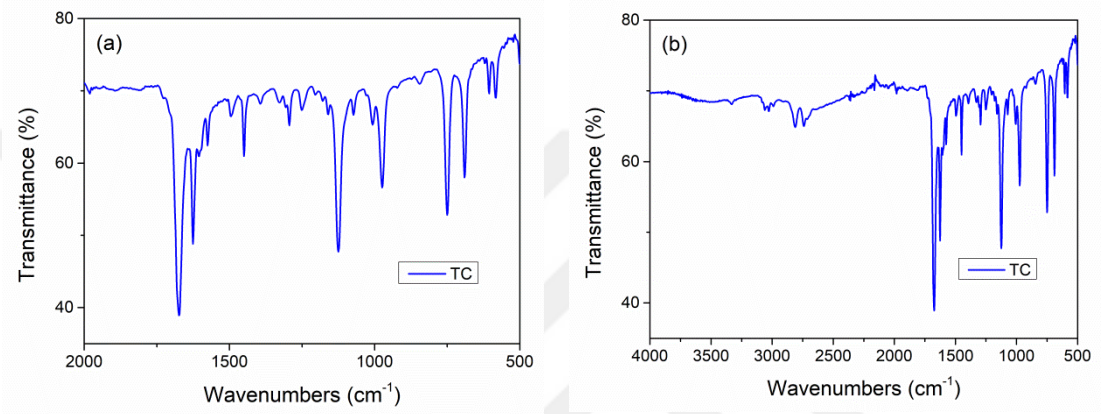

Figure 3.14 : FTIR spectrum of *trans*-cinnamaldehyde in the interval of wavenumbers between 500-2000 cm^{-1} (a) and 500-4000 cm^{-1} (b)

A strong peak observed at 1673 cm^{-1} is related to the carbonyl group (C=O) of TC. Peaks in 1400-1630 cm^{-1} range might be attributed to C=C bonds. The peak at 2810 cm^{-1} is due to the aliphatic C-H bonds and the peak that appeares around 3000 cm^{-1} can correspond to aromatic C-H bonds. TC loaded CC-3v2 particles were subjected to FTIR analysis with its control group which is empty CC-1v2 particles. FTIR spectra of above mentioned particles are shown in Figure 3.15.

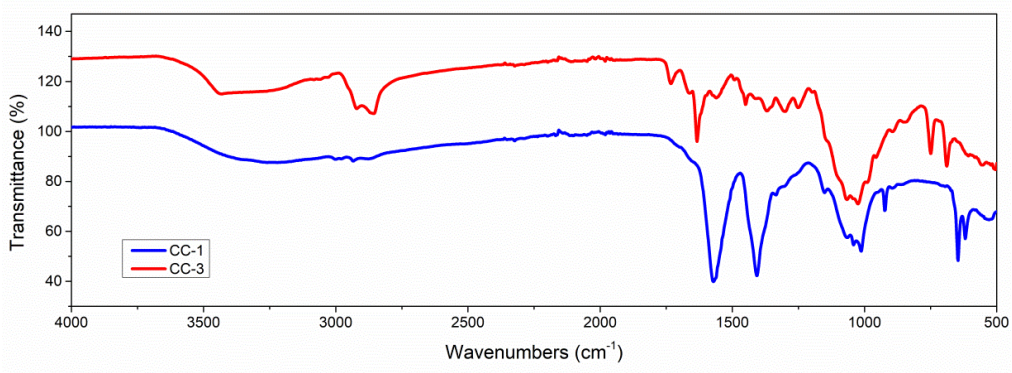

Figure 3.15 : FTIR spectra of empty CC-1v2 and TC loaded CC-3v2 particles

Chitosan, xanthan gum and dialdehyde xanthan gum were also analyzed using FTIR measuments in order to have proper knowledge about the synthesized system. As can be seen in Figure 3.15 and Figure 3.16, the peak that was previously observed from FTIR spectra of DXG due to aldehyde absorbance at 1722 $cm^{-1}$was disappeared in the CC-1v2 spectrum. CC-1v2 particles contain only CH and DXG in their formulation.

Furthermore, it was also expected to see a peak around 1600-1630 cm^{-1} that related to stretching vibration of the C=N group belonging to imine bonds which can verify the cross-linking between amine groups of CH and aldehyde groups of DXG. On the other hand, CH also has a peak around 1644 cm^{-1} that corresponded to in-plane bending vibrations of the amine groups ($–NH_2$). It seems from Fig. 3.15 and spectrum of CC-1v2 that both imine and amine bands were screened by the strong peak at 1571 cm^{-1} due to the interaction of CH with DXG both ionically and covalently.

However, TC has also aldehyde groups in its structure which demonstrates itself at 1673 cm^{-1} due to C=O stretching. The peaks around 1560 $cm^{-1}$and 1670 cm^{-1} of CC-3v2 may be related to TC loading. The new peak occurred at 1732 cm^{-1} may be a result of a shifting due to the existence of aldehyde of TC.

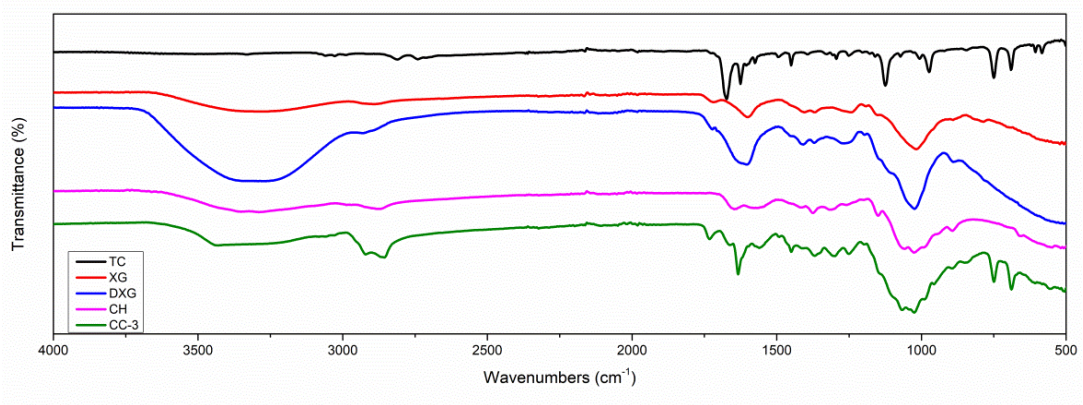

Figure 3.16 : FTIR spectra of CC-3v2 microparticles and their assembly components

The aldehyde group of TC can play an extra role in terms of cross-linking of chitosan [93]. This possibility was tried to keep low by making arrangements on synthesis procedure and conditions of particles during this study. In this study, cross-linking possibility of chitosan by TC was verified by release studies of TC loaded microparticles.

3.1.1.5 DSC analysis

In order to examine possible differences that may have been created by dual cross-linking of CH, CC-3v2 and CC-4v2 particles have been subjected to DSC analysis with their assembly components.

Structural features, hydrophilic properties and polymer-polymer, polymer-active molecule interactions can be examined by determining endothermal and exothermal peaks of the DSC diagram as shown in Figure 3.17.

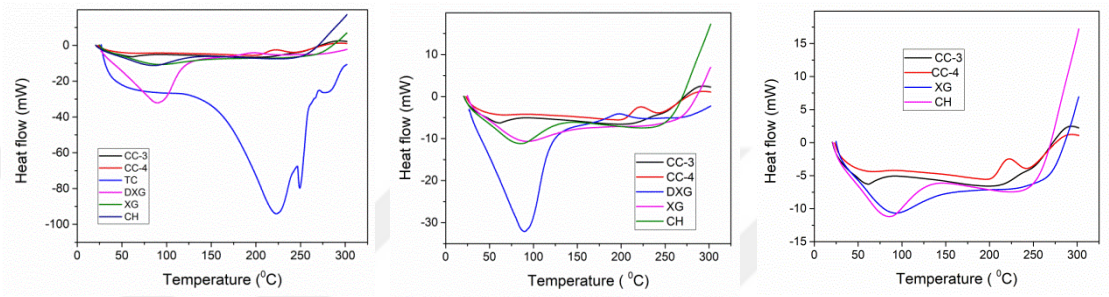

Figure 3.17 : DSC diagram of microparticles and their assembly components

The endothermic peak observed around 80-100 ^{o}C should be related to water loss for particles and polymers. As can be shown in Figure 3.17 most strong peak belongs to DXG due to water loss. After the encapsulation of TC, it loses its strong endothermic peak around 248 ^{o}C that exhibits due to its boiling point and potential hydrolysis of TC [94]. The disappearence of this peak can confirm the encapsulation of TC into microparticles. The exothermic peak of CC-4v2 that can be seen around 225 ^{o}C, may be related to the crystalline nature of microparticles due to NaTPP cross-linking [95].

The exotherm behavior around 200 ^{o}C can be caused by the glass transition state of chitosan. CC-4v2 formulation also consists of electrostatic interactions which require less energy to be interrupted. The CC-3v2 has covalent bonding and electrostatic interactions due to its constituent polymers. However, the DSC diagram of CC-3v2 employed slightly more energy compared to CC-4v2. The reason behind this situation can be related to NaTPP interaction in CC-4v2 formulation which prevents imine bonding for some of the amine groups of chitosan.

3.1.1.6 SEM analysis

In order to determine their surface morphology, TC-loaded microparticles were examined by SEM.

Microphotographs of CC-3v2, CC-4v2, IC-3v2 and IC-4v2 can be seen in Figure 3.18 and Figure 3.19 below.

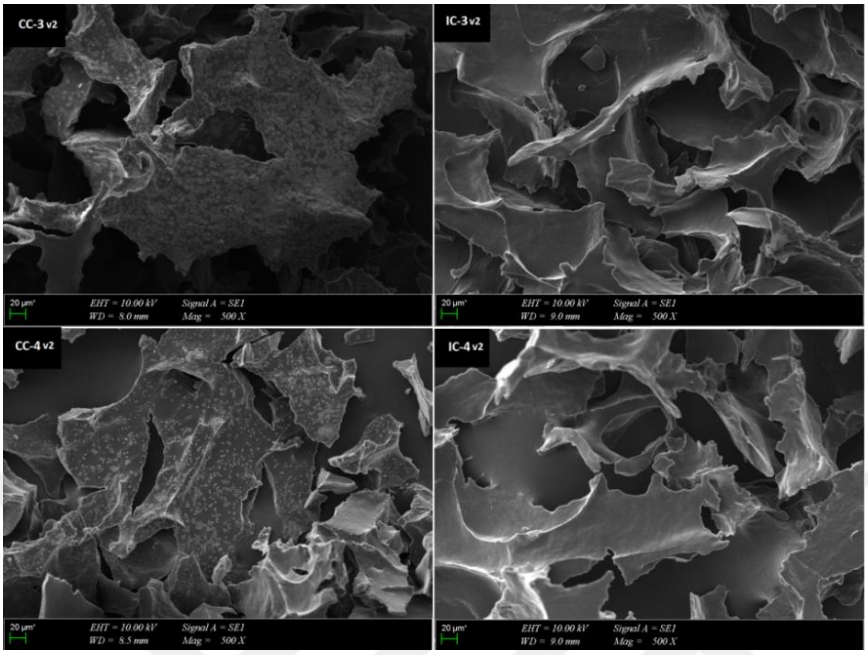

Figure 3.18 : Surface morphology comparison of microparticles.

According to SEM images, the surface roughness of CC-3v2 and CC-4v2 particles was higher compared to IC-3v2 and IC-4v2 microparticles. TC-loaded IC group exhibited more smoothness in their surfaces. Aldehyde cross-linking of chitosan may have caused a roughness on the surfaces of the CC group [97]. Cross-linking degree and degree of acetylation of chitosan can affect the size and morphology of particles.

On the other hand, all particles have exhibited non-uniform, shapeless structures. This situation can be related to the homogenization process during synthesis of particles.

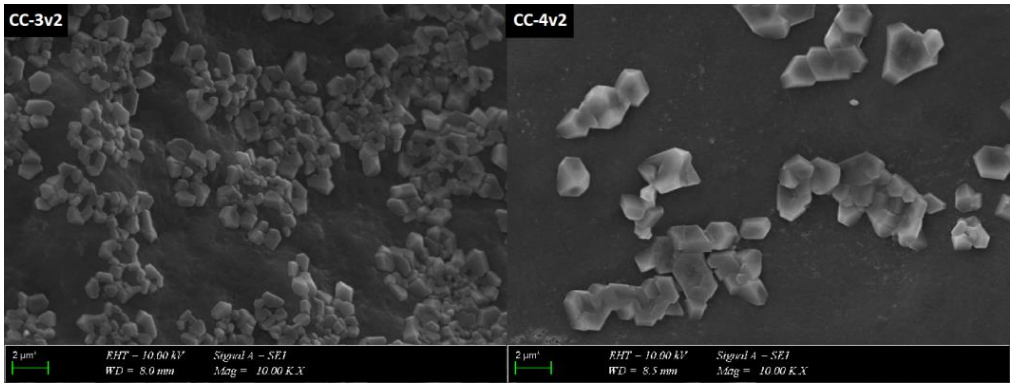

Figure 3.19 : SEM images of TC-loaded CC-3v2 and CC-4v2 particles.

It has been observed that CC-3v2 and CC-4v2 particles have crystalline structures on their surface. This can be due to the crystalization of TC which could be entrapped on the outer surface of particles. However, in the IC group, there was no crystalline structure observed on the surfaces of microparticles.

Crystalline structures on the surface of the CC group may also be caused by NaOH which was used to adjust the final pH of formulations before the reaction ended. The particle sizes of synthesized particles were also verified by SEM images.

3.1.1.7 In-vitro release studies

Preliminary release study was conducted for the first versions; IC-3v1 and CC-3v1 formulations to gain information about their release behaviour in neutral pH at 25^{o}C. 10 mg samples, containing approximately 3.0 mg and 6.0 mg of TC, respectively, for each formulation, were weighed and transferred into 30 ml of 10 mM PBS buffer at pH 7.0 . Cumulative release of first versions were shown in Figure 3.20.

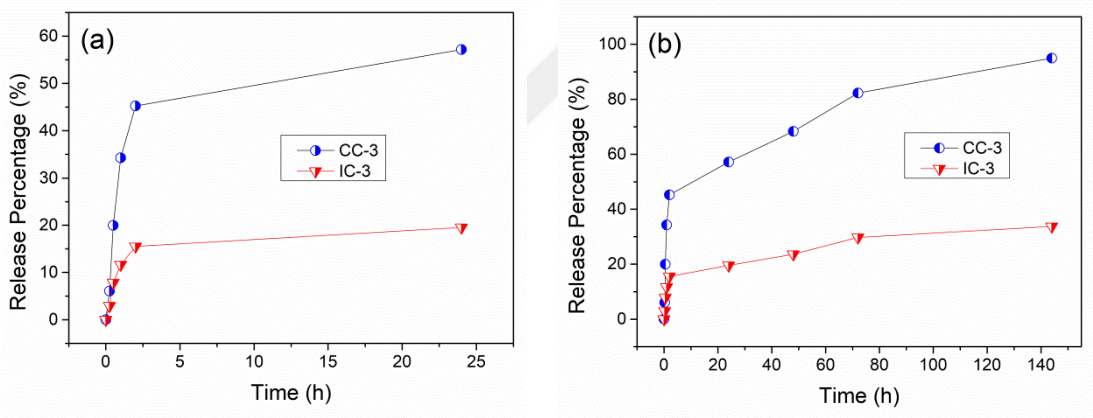

Figure 3.20 : Cumulative release profile of IC-3v1 and CC-3v1 in the time interval of 0-24h (a) and 0-144h(b) in 10 mM PBS buffer at pH 7.0 and at 25^{o}C.

As can be seen in Figure 3.20(a), the release rate was very fast for the first 3 hours which can be considered a burst release. CC-3v1 was shown superior release behaviour compared to IC-3v1. This can be related to the swelling capacity of CC-3v1 due to its gel formation. On the other hand, the release behaviour of IC-3v1 can be more related to degradation than swelling.

In this study, the first six hours and 24 hours of release behaviours of the generated system are critical due to simulating the release time a drug formulation spent in the gastrointestinal tract of the human body. However preliminary release study was

conducted until 144 hours to get the information about release behaviour of generated systems. Results have shown that the CC-3v1 system can release all TC molecules that it theoretically possesses. This result can be also considered as proof that chitosan in the CC-3v1 system was not cross-linked by aldehyde groups of TC.

The abovementioned preliminary release study confirmed that it can be expected to observe a higher release profile for CC-3v2 formulation at neutral pH which simulates instestinal fluid in this study.

Final versions of synthesized particles were subjected to release experiment at acidic and neutral pHs. 25 mg of CC-3v2, CC-4v2and IC-3v2 were weighed as duplicates and transferred into 25 ml of 10 mM PBS buffers at pH 2.0 and pH 7.0 of 37^{o}C. The temperature of 37^{o}C was selected for mimicking the body temperature. According to their loading capacities, they should have 10.89, 10.76 and 11.23 mg of *trans*-cinnamaldehyde (TC), respectively.

Release profiles of particles are shown in Figure 3.21 and Figure 3.22.

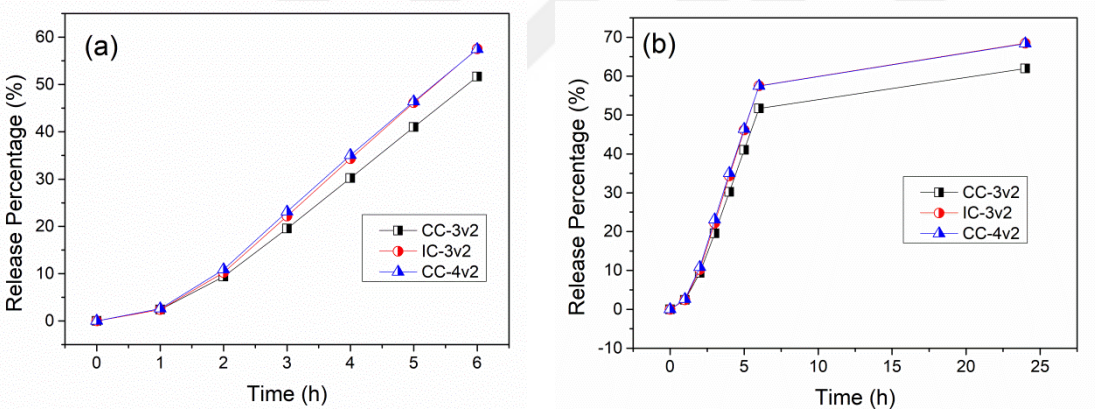

Figure 3.21 : Release profiles of CC-3v2, CC-4v2 and IC-3v2 in the time interval of 0-6h (a) and 0-24(b) in 10 mM PBS buffer at pH 2.0 and at 37^{o}C.

CC-4v2 particles were selected as a second control of this release study to gain information about effect of ionic cross-linking on release behaviour of particles. According to release profiles, NaTPP has an effect on release of TC from CC-4v2 particles. This can be due to occupying amine groups of chitosan that limits the imine formation with DXG. As can be seen in the Figure 3.21, CC-3v2 particles has the slowest release in acidic pH as expected. However, the gap between CC-3v2 and other selected particles was observed as quite low. At the end of 6th hour, other two

control groups have released 57 % of their loaded TC, CC-3v2 has released 51.6 % of its loaded TC.

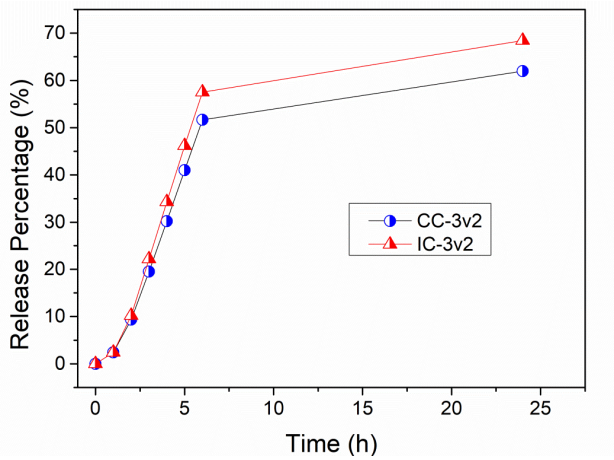

Figure 3.22 : Cumulative release profiles of CC-3v2 and IC-3v2 in the time interval of 0-24h 10 mM PBS buffer at pH 2.0 and at 37°C.

Even if these results confirm the hypothesis of this study, further optimization is required for the CC-3v2 system. The slow release of CC-3v2 should be related to its covalent cross-linking, however, its close gap to other formulations can be a result of low chemical cross-linking. It can be said that the release behaviour of all particles in this buffer is dominantly based on degradation due to protonated free amine groups of chitosan.

Release studies at neutral pH were conducted in PBS buffer at pH 7.0 to simulate intestinal fluid conditions. Release profiles of particles are shown in Figure 3.23 and Figure 3.24.

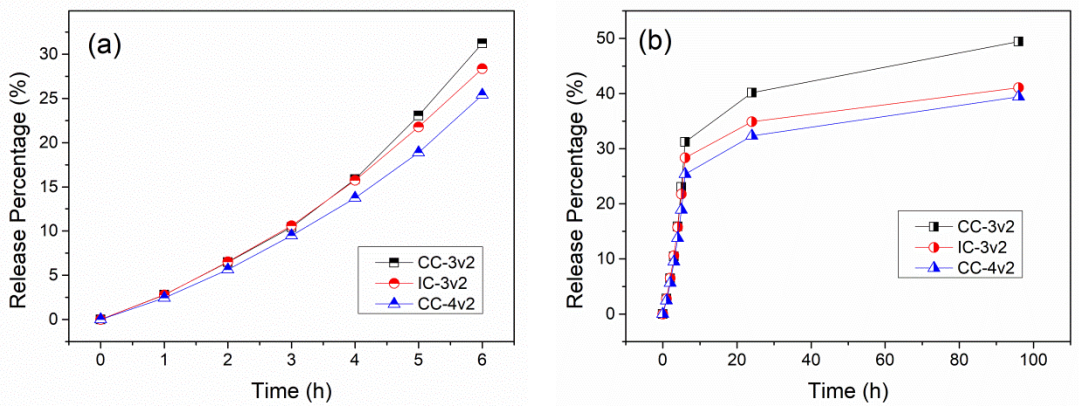

Figure 3.23 : Release profiles of CC-3v2, CC-4v2 and IC-3v2 in the time interval of 0-6h and 0-96h 10 mM PBS buffer at pH 7.0 and at 37°C.

CC-3v2 particles have released 31.21 % of their loaded TC molecules within 6 hours. On the other hand, CC-4v2 and IC-3v2 particles have released 25.38 % and 28.36 % of their loaded TC molecules during the first 6 hours, respectively. This can be due to the swelling behavior of CC-3v2 particles that were more dominant compared to the other two formulations. The release behaviour of all particles exhibited a slow release rate at pH 7.0. It can be stated that possible degradation-based release of the particles, which demonstrated itself at pH 2.0, did not play a dominant role in neutral pH. Even if these results confirm the hypothesis of this study, further optimization is required for the CC-3v2 system.

CC-3v2 particles have released 40.1 % of loaded TC while IC-3v2 particles have released 34.9 % at the end of the 24th hour of the release study. However, CC-3v2, CC-4v2 and IC-3v2 have released 49.45 %, 39.4 % and 41.06 % TC, respectively at the 96th hour of the release study. These results can suggest that the release rate of CC-3v2 particles has increased over time. CC-4v2 particles have both ionic and covalent cross-linker in their system which can negatively affect their swelling behaviour due to excessive cross-linking.

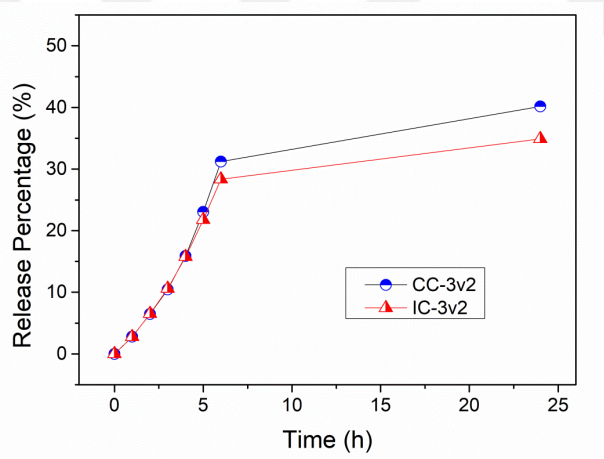

Figure 3.24 : Cumulative release profiles of CC-3v2 and IC-3v2 in the time interval of 0-24h 10 mM PBS buffer at pH 7.0 and at 37^{o}C.

DXG and XG can exhibit swelling behaviour in aqueous buffers. The optimized concentration of these polymers in developed microparticles was 0.15 %. The low concentration of these polymers decreased the swelling behaviour of the system for all particles. This suggestion can be verified by the release behaviour of first version of the developed systems which both consist of 0.7 % of XG and DXG.

4. CONCLUSION AND FUTURE PERSPECTIVE

In this thesis, xanthan gum (XG) was modified via sodium periodate oxidation to obtain dialdehyde xanthan gum (DXG) which is natural polymer, with the covalent cross-linker ability for chitosan. The oxidization degree of DXG was found to be 29.4 % and DXG was utilized to form a non-toxic biopolymer-based matrice with chitosan (CH) which can be employed for drug delivery applications.

Trans-cinnamaldehyde was successfully encapsulated into created matrice and the process was optimized to obtain microparticles. Synthesized particles were characterized in terms of their encapsulation efficiency, size, morphology, chemical structure and release behaviour.

Trans-cinnamaldehyde loaded dialdehyde xanthan gum-chitosan microparticles have been shown 80.1 % encapsulation efficiency, over 6 μm size with 0.310 PDI value. Loading of *trans*-cinnamaldehyde into synthesized particles has been proved via FTIR and DSC analysis. The surface roughness of particles has been demonstrated by SEM measurements. The release profile of synthesized CH-DXG microparticles indicated the particles have shown slower release in acidic conditions and faster release in neutral conditions compared to their control groups.

This study proves that developed biopolymeric-based CH-DXG matrices with non-toxic drug carriers can be used in the safe delivery of antimicrobial *trans*-cinnamaldehyde through the gastrointestinal tract which can demonstrate acidic and neutral conditions in different regions.

After a detailed antimicrobial study of the synthesized drug delivery system against human pathogens in the gastrointestinal tract has been carried out, it is thought that this proposed system can replace or synergistically use with traditional antibiotics in the future.

REFERENCES

[1] **Tiwari, G., et al.,** *Drug delivery systems: An updated review.* International journal of pharmaceutical investigation, 2012. **2**(1): p. 2-11.

[2] **Ochekpe**, **N.A., P.O. Olorunfemi, and N.C. Ngwuluka**, *Nanotechnology and drug delivery part 2: nanostructures for drug delivery.* Tropical Journal of Pharmaceutical Research, 2009. **8**(3).

[3] **Liu, D**., **et al.**, *The Smart Drug Delivery System and Its Clinical Potential.* Theranostics, 2016. **6**(9): p. 1306-1323.

[4] **Kumari, A., S.K. Yadav, and S.C. Yadav**, *Biodegradable polymeric nanoparticles based drug delivery systems.* Colloids and Surfaces B: Biointerfaces, 2010. **75**(1): p. 1-18.

[5] **Rossi, F., et al.,** *Polymer hydrogel functionalized with biodegradable nanoparticles as composite system for controlled drug delivery.* Nanotechnology, 2014. **26**(1): p. 015602.

[6] **Nayak, A.K. and M.S. Hasnain,** *Plant polysaccharides in drug delivery applications*, in *Plant polysaccharides-based multiple-unit systems for oral drug delivery*. 2019, Springer. p. 19-23.

[7] **Hasnain**, **M.S., et al.,** *Biopolymers for Drug Delivery*, in *Advanced Biopolymeric Systems for Drug Delivery*, A.K. Nayak and M.S. Hasnain, Editors. 2020, Springer International Publishing: Cham. p. 1-29.

[8] **Qiu, L.Y. and Y.H. Bae,** *Polymer Architecture and Drug Delivery.* Pharmaceutical Research, 2006. **23**(1): p. 1-30.

[9] **Shariatinia, Z.,** *Chapter 2 - Pharmaceutical applications of natural polysaccharides*, in *Natural Polysaccharides in Drug Delivery and Biomedical Applications*, M.S. Hasnain and A.K. Nayak, Editors. 2019, Academic Press. p. 15-57.

[10] **Delcassian, D., et al.,** *Drug delivery across length scales.* Journal of Drug Targeting, 2019. **27**(3): p. 229-243.

[11] **Yadav, H.K.S., et al.,** *Chapter 17 - Polymer-Based Nanomaterials for Drug-Delivery Carriers*, in *Nanocarriers for Drug Delivery*, S.S. Mohapatra, et al., Editors. 2019, Elsevier. p. 531-556.

[12] **Cho, K., et al.,** *Therapeutic nanoparticles for drug delivery in cancer.* Clinical cancer research, 2008. **14**(5): p. 1310-1316.

[13] **Jones, M.-C. and J.-C. Leroux**, *Polymeric micelles–a new generation of colloidal drug carriers.* European journal of pharmaceutics and biopharmaceutics, 1999. **48**(2): p. 101-111.

[14] **Procopio, A., et al.**, *Recent Fabrication Methods to Produce Polymer-Based Drug Delivery Matrices (Experimental and In Silico Approaches).* Pharmaceutics, 2022. **14**(4): p. 872.

[15] **Bennet, D. and S. Kim**, *Polymer nanoparticles for smart drug delivery*. Vol. 8. 2014: chapter.

[16] **Nagavarma, B., et al.**, *Different techniques for preparation of polymeric nanoparticles-a review.* Asian j pharm clin res, 2012. **5**(3): p. 16-23.

[17] **Safari, J. and Z. Zarnegar**, *Advanced drug delivery systems: Nanotechnology of health design A review.* Journal of Saudi Chemical Society, 2014. **18**(2): p. 85-99.

[18] **Gupta, U., et al.**, *A review of in vitro–in vivo investigations on dendrimers: the novel nanoscopic drug carriers.* Nanomedicine: Nanotechnology, Biology and Medicine, 2006. **2**(2): p. 66-73.

[19] **Newkome, G.R., et al.**, *Dendrimers and dendrons: concepts, syntheses, applications*. Vol. 623. 2001: Wiley Online Library.

[20] **Thwala, L.N.**, *Preparation and characterization of alginate-chitosan nanoparticles as a drug delivery system for lipophilic compounds*. 2012: University of Johannesburg (South Africa).

[21] **Nayak, A.K., M.S. Hasnain, and T.M. Aminabhavi**, *Drug delivery using interpenetrating polymeric networks of natural polymers: A recent update.* Journal of Drug Delivery Science and Technology, 2021. **66**: p. 102915.

[22] **Pal, D. and A.K. Nayak**, *Plant Polysaccharides Blended Ionotropically Gelled Alginate Multiple Unit Systems for Sustained Drug Release*, in *Handbook of Composites from Renewable Materials*. 2017. p. 399-440.

[23] **Matricardi, P., et al.**, *Interpenetrating Polymer Networks polysaccharide hydrogels for drug delivery and tissue engineering.* Advanced Drug Delivery Reviews, 2013. **65**(9): p. 1172-1187.

[24] **Nayak, A.K. and D.K. Pal**, *Chitosan-based Interpenetrating Polymeric Network Systems for Sustained Drug Release*, in *Advanced Theranostic Materials*. 2015. p. 183-208.

[25] **Farooq, U., J. Teuwen, and C. Dransfeld**, *Toughening of Epoxy Systems with Interpenetrating Polymer Network (IPN): A Review.* Polymers, 2020. **12**: p. 1908.

[26] **Li, D., et al.**, *Polyelectrolyte Complex-Covalent Interpenetrating Polymer Network Hydrogels.* 2022.

[27] **Liu, L., et al.**, *Hydrogels from Biopolymer Hybrid for Biomedical, Food, and Functional Food Applications.* Polymers, 2012. **4**: p. 997-1011.

[28] **Jana, S., et al.**, *Aceclofenac-loaded chitosan-tamarind seed polysaccharide interpenetrating polymeric network microparticles.* Colloids and Surfaces B: Biointerfaces, 2013. **105**: p. 303-309.

[29] **Jana, S., K.K. Sen, and S.K. Basu**, *In vitro aceclofenac release from IPN matrix tablets composed of chitosan-tamarind seed polysaccharide.*

International Journal of Biological Macromolecules, 2014. **65**: p. 241-245.

[30] **Bulut, E.**, *In-Vitro Evaluation of Ibuprofen-Loaded Microspheres Prepared from Novel Chitosan/Poly(vinyl alcohol) Interpenetrating Polymer Network.* Polymer-Plastics Technology and Engineering, 2014. **53**(4): p. 371-378.

[31] **Xinxin, S., et al.**, *Preparation of Drug-Eluting Microspheres Based on Semi-Interpenetrating Polymer Network of Modified Chitosan and Poly(2-acrylamide-2-methylpropanesulfonic acid).* Polymer Science, Series A, 2019. **61**(1): p. 61-69.

[32] **Ullah, F., et al.**, *Synthesis and functionalization of chitosan built hydrogel with induced hydrophilicity for extended release of sparingly soluble drugs.* Journal of Biomaterials Science, Polymer Edition, 2018. **29**(4): p. 376-396.

[33] **Puertas-Bartolomé, M.**, et al., *Bioadhesive functional hydrogels: Controlled release of catechol species with antioxidant and antiinflammatory behavior*. Materials Science and Engineering: C, 2019. **105**: p. 110040.

[34] **Anwar, M., et al.**, *Formulation and evaluation of interpenetrating network of xanthan gum and polyvinylpyrrolidone as a hydrophilic matrix for controlled drug delivery system.* Polymer Bulletin, 2021. **78**(1): p. 59-80.

[35] **Ray, S., et al.**, *Novel interpenetrating network microspheres of xanthan gum–poly(vinyl alcohol) for the delivery of diclofenac sodium to the intestine—in vitro and in vivo evaluation.* Drug Delivery, 2010. **17**(7): p. 508-519.

[36] **Giri, T.K.**, *20 - Alginate Containing Nanoarchitectonics for Improved Cancer Therapy*, in *Nanoarchitectonics for Smart Delivery and Drug Targeting*, A.M. Holban and A.M. Grumezescu, Editors. 2016, William Andrew Publishing. p. 565-588.

[37] **Ahirrao, S.P., et al.**, *Ionotropic gelation: a promising cross linking technique for hydrogels.* J. Pharm. Nanotechnol, 2014. **2**: p. 1-6.

[38] **Pedroso-Santana, S. and N. Fleitas-Salazar**, *Ionotropic gelation method in the synthesis of nanoparticles/microparticles for biomedical purposes.* Polymer International, 2020. **69**(5): p. 443-447.

[39] **Patil, P., D. Chavanke, and M. Wagh**, *A review on ionotropic gelation method: Novel approach for controlled gastroretentive gelispheres.* International Journal of Pharmacy and Pharmaceutical Sciences, 2012. **4**: p. 27-32.

[40] **Wu, J., et al.**, *Preparation and biological activity studies of resveratrol loaded ionically cross-linked chitosan-TPP nanoparticles.* Carbohydr Polym, 2017. **175**: p. 170-177.

[41] **Delaney, K.T. and G.H. Fredrickson**, *Theory of polyelectrolyte complexation—Complex coacervates are self-coacervates.* The Journal of Chemical Physics, 2017. **146**(22): p. 224902.

[42] **Sæther, H.V., et al.**, *Polyelectrolyte complex formation using alginate and chitosan.* Carbohydrate Polymers, 2008. **74**(4): p. 813-821.

[43] **Espinosa-Andrews, H., et al.**, *Gum arabic− chitosan complex coacervation.* Biomacromolecules, 2007. **8**(4): p. 1313-1318.

[44] **Astete, C.E., et al.**, *Ca2+ cross-linked alginic acid nanoparticles for solubilization of lipophilic natural colorants.* Journal of Agricultural and Food Chemistry, 2009. **57**(16): p. 7505-7512.

[45] **Dhakal, S. and J. He**, *Microencapsulation of Vitamins in Food Applications to Prevent Losses in Processing and Storage: A Review*. Food Research International, 2020. **137**: p. 109326.

[46] **Timilsena, Y.P., et al.**, *Complex coacervation: Principles, mechanisms and applications in microencapsulation.* International Journal of Biological Macromolecules, 2019. **121**: p. 1276-1286.

[47] **Reis, C.P., et al.**, *Nanoencapsulation I. Methods for preparation of drug-loaded polymeric nanoparticles.* Nanomedicine: Nanotechnology, Biology and Medicine, 2006. **2**(1): p. 8-21.

[48] **Dubey, S., et al.**, *Chapter 4 - Nanobiomaterials: Novel nanoplatforms for protein and peptide delivery*, in *Nanobiomaterials in Drug Delivery*, A.M. Grumezescu, Editor. 2016, William Andrew Publishing. p. 111-146.

[49] **Zielińska, A., et al.**, *Polymeric Nanoparticles: Production, Characterization, Toxicology and Ecotoxicology.* Molecules, 2020. **25**: p. 3731.

[50] **Saikia, C. and P. Gogoi**, *Chitosan: A Promising Biopolymer in Drug Delivery Applications.* Journal of Molecular and Genetic Medicine, 2015. **s4**.

[51] **Zhu, Y., Y. Liu, and Z. Pang**, *Chapter 4 - Chitosan in drug delivery applications*, in *Natural Polysaccharides in Drug Delivery and Biomedical Applications*, M.S. Hasnain and A.K. Nayak, Editors. 2019, Academic Press. p. 101-119.

[52] **Kaur, S. and G.S. Dhillon**, *The versatile biopolymer chitosan: potential sources, evaluation of extraction methods and applications.* Crit Rev Microbiol, 2014. **40**(2): p. 155-75.

[53] **Dutta, P.K., J. Dutta, and V. Tripathi**, *Chitin and chitosan: Chemistry, properties and applications.* 2004.

[54] **Yi, H., et al.**, *Biofabrication with chitosan.* Biomacromolecules, 2005. **6**(6): p. 2881-2894.

[55] **Aranaz, I., et al.**, *Chitosan: An Overview of Its Properties and Applications.* Polymers, 2021. **13**(19): p. 3256.

[56] **Kaczmarek, M.B., et al.**, *Enzymatic modifications of chitin, chitosan, and chitooligosaccharides.* Frontiers in bioengineering and biotechnology, 2019: p. 243.

[57] **Islam, S., M. Bhuiyan, and M. Islam**, *Chitin and chitosan: structure, properties and applications in biomedical engineering.* Journal of Polymers and the Environment, 2017. **25**(3): p. 854-866.

[58] **Brasselet, C., et al.**, *Modification of chitosan for the generation of functional derivatives.* Applied Sciences, 2019. **9**(7): p. 1321.

[59] **Rafique, A., et al.**, *International Journal of Biological Macromolecules Chitosan functionalized poly (vinyl alcohol) for prospects biomedical and industrial applications: A review.* Int. J. Biol. Macromol., 2016. **87**: p. 141-154.

[60] **Jayakumar, R., et al.**, *Biomedical applications of chitin and chitosan based nanomaterials—A short review.* Carbohydrate polymers, 2010. **82**(2): p. 227-232.

[61] **Laroche, C., et al.**, *Bioactivity of chitosan and its derivatives.* Current Organic Chemistry, 2018. **22**(7): p. 641-667.

[62] **Pellá, M.C., et al.**, *Chitosan-based hydrogels: From preparation to biomedical applications.* Carbohydrate Polymers, 2018. **196**: p. 233-245.

[63] **Hussein, K., et al.**, *New insights into the pros and cons of cross-linking decellularized bioartificial organs.* The International journal of artificial organs, 2017. **40**.

[64] **Öztop, H.N., D. Saraydin, and Ş. Cetinus**, *pH-sensitive chitosan films for baker's yeast immobilization.* Applied biochemistry and biotechnology, 2002. **101**(3): p. 239-249.

[65] **Jóźwiak, T., et al.**, *Effect of ionic and covalent crosslinking agents on properties of chitosan beads and sorption effectiveness of Reactive Black 5 dye.* Reactive and Functional Polymers, 2017. **114**: p. 58-74.

[66] **Silvestro, I., et al.**, *Preparation and characterization of TPP-chitosan crosslinked scaffolds for tissue engineering.* Materials, 2020. **13**(16): p. 3577.

[67] **Wang, W., R. Narain, and H. Zeng**, *Chapter 10 - Hydrogels*, in *Polymer Science and Nanotechnology*, R. Narain, Editor. 2020, Elsevier. p. 203-244.

[68] **Wei, Z., et al.**, *Self-healing gels based on constitutional dynamic chemistry and their potential applications.* Chemical Society Reviews, 2014. **43**(23): p. 8114-8131.

[69] **Gupta, B., et al.**, *Preparation and characterization of in-situ crosslinked pectin–gelatin hydrogels.* Carbohydrate Polymers, 2014. **106**: p. 312-318.

[70] **Huang, J., S. Zajforoushan Moghaddam, and E. Thormann**, *Structural Investigation of a Self-Cross-Linked Chitosan/Alginate Dialdehyde Multilayered Film with in Situ QCM-D and Spectroscopic Ellipsometry.* ACS Omega, 2019. **4**(1): p. 2019-2029.

[71] **Sen, S.O., et al.**, *DEVELOPMENT AND EVALUATION OF SUSTAIN RELEASE MICROPARTICLES OF METOPROLOL SUCCINATE.* International Journal of Applied Pharmaceutics, 2019. **11**(5): p. 166-172.

[72] **Maiti, S., et al.**, *Physical and self–crosslinking mechanism and characterization of chitosan-gelatin-oxidized guar gum hydrogel.* Polymer Testing, 2021. **97**: p. 107155.

[73] **Hublik, G.**, *10.11 - Xanthan*, in *Polymer Science: A Comprehensive Reference*, K. Matyjaszewski and M. Möller, Editors. 2012, Elsevier: Amsterdam. p. 221-229.

[74] **Petri, D.F.S.**, *Xanthan gum: A versatile biopolymer for biomedical and technological applications.* Journal of Applied Polymer Science, 2015. **132**(23).

[75] **Abu Elella, M.H., et al.**, *Xanthan gum-derived materials for applications in environment and eco-friendly materials: A review.* Journal of Environmental Chemical Engineering, 2021. **9**(1): p. 104702.

[76] **Singhvi, G., et al.**, *Chapter 5 - Xanthan gum in drug delivery applications*, in *Natural Polysaccharides in Drug Delivery and Biomedical Applications*, M.S. Hasnain and A.K. Nayak, Editors. 2019, Academic Press. p. 121-144.

[77] **Argin, S., P. Kofinas, and Y.M. Lo**, *The cell release kinetics and the swelling behavior of physically crosslinked xanthan–chitosan hydrogels in simulated gastrointestinal conditions.* Food Hydrocolloids, 2014. **40**: p. 138-144.

[78] **Patel, J., et al.**, *Xanthan gum derivatives: Review of synthesis, properties and diverse applications.* RSC Advances, 2020. **10**(45): p. 27103-27136.

[79] **Ngwabebhoh, F.A., et al.**, *Self-crosslinked chitosan/dialdehyde xanthan gum blended hypromellose hydrogel for the controlled delivery of ampicillin, minocycline and rifampicin.* International Journal of Biological Macromolecules, 2021. **167**: p. 1468-1478.

[80] **Birk, S.E., A. Boisen, and L.H. Nielsen**, *Polymeric nano- and microparticulate drug delivery systems for treatment of biofilms.* Advanced Drug Delivery Reviews, 2021. **174**: p. 30-52.

[81] **Amalaradjou Mary Anne, R., et al.**, *Antibiofilm Effect of Trans-Cinnamaldehyde on Uropathogenic Escherichia coli.* Journal of Urology, 2010. **184**(1): p. 358-363.

[82] **Gomes, C., R.G. Moreira, and E. Castell-Perez**, *Poly (DL-lactide-co-glycolide)(PLGA) nanoparticles with entrapped trans-cinnamaldehyde and eugenol for antimicrobial delivery applications.* Journal of Food Science, 2011. **76**(2): p. N16-N24.

[83] **Lee, J.-E., et al.**, *Antibacterial mode of action of trans-cinnamaldehyde derived from cinnamon bark (Cinnamomum verum) essential oil against Agrobacterium tumefaciens.* Pesticide Biochemistry and Physiology, 2020. **165**: p. 104546.

[84] **Cheng, Q., et al.**, *The Intestinal Cinnamaldehyde Release and Antioxidative Capacity of Broiler Chickens Fed Diets Supplemented with Coated Oleum Cinnamomi.* Journal of Applied Poultry Research, 2019. **28**(4): p. 1058-1068.

[85] **Doyle, A.A. and J.C. Stephens**, *A review of cinnamaldehyde and its derivatives as antibacterial agents.* Fitoterapia, 2019. **139**: p. 104405.

[86] **Do, J., et al.**, *Trans-Cinnamaldehyde Alleviates Amyloid-Beta Pathogenesis via the SIRT1-PGC1α-PPARγ Pathway in 5XFAD Transgenic Mice.* International Journal of Molecular Sciences, 2020. **21**: p. 4492.

[87] **Saka, R. and N. Chella**, *Nanotechnology for delivery of natural therapeutic substances: a review.* Environmental Chemistry Letters, 2021. **19**(2): p. 1097-1106.

[88] **Zuo, Y., et al.**, *Preparation and characterization of dialdehyde starch by one-step acid hydrolysis and oxidation.* International Journal of Biological Macromolecules, 2017. **103**: p. 1257-1264.

[89] **Argin-Soysal, S., P. Kofinas, and Y.M. Lo**, *Effect of complexation conditions on xanthan–chitosan polyelectrolyte complex gels.* Food hydrocolloids, 2009. **23**(1): p. 202-209.

[90] **Osiro, D., R. Franco, and L. Colnago**, *Spectroscopic Characterization of the Exopolysaccharide of Xanthomonas axonopodis pv. citri in Cu2+ Resistance Mechanism.* Journal of the Brazilian Chemical Society, 2011. **22**: p. 1339-1345.

[91] **Malik, N.S., et al.**, *Chitosan/xanthan gum based hydrogels as potential carrier for an antiviral drug: fabrication, characterization, and safety evaluation.* Frontiers in chemistry, 2020: p. 50.

[92] **Williams, P.M.**, *Zeta Potential*, in *Encyclopedia of Membranes*, E. Drioli and L. Giorno, Editors. 2016, Springer Berlin Heidelberg: Berlin, Heidelberg. p. 2063-2064.

[93] **Gadkari, R., et al.**, *Green Synthesis of chitosan-cinnamaldehyde cross-linked nanoparticles: characterization and antibacterial activity.* Carbohydrate Polymers, 2019. **226**: p. 115298.

[94] **Teixeira, B.N., et al.**, *Synthesis and characterization of nano-encapsulated black pepper oleoresin using hydroxypropyl beta-cyclodextrin for antioxidant and antimicrobial applications.* Journal of Food Science, 2013. **78**(12): p. N1913-N1920.

[95] **Bhumkar, D. and V. Pokharkar**, *Studies on effect of pH on cross-linking of Chitosan with sodium tripolyphosphate: A technical note.* AAPS PharmSciTech, 2006. **7**: p. E50.

APPENDICES

APPENDIX A: Figures and Table

APPENDIX A

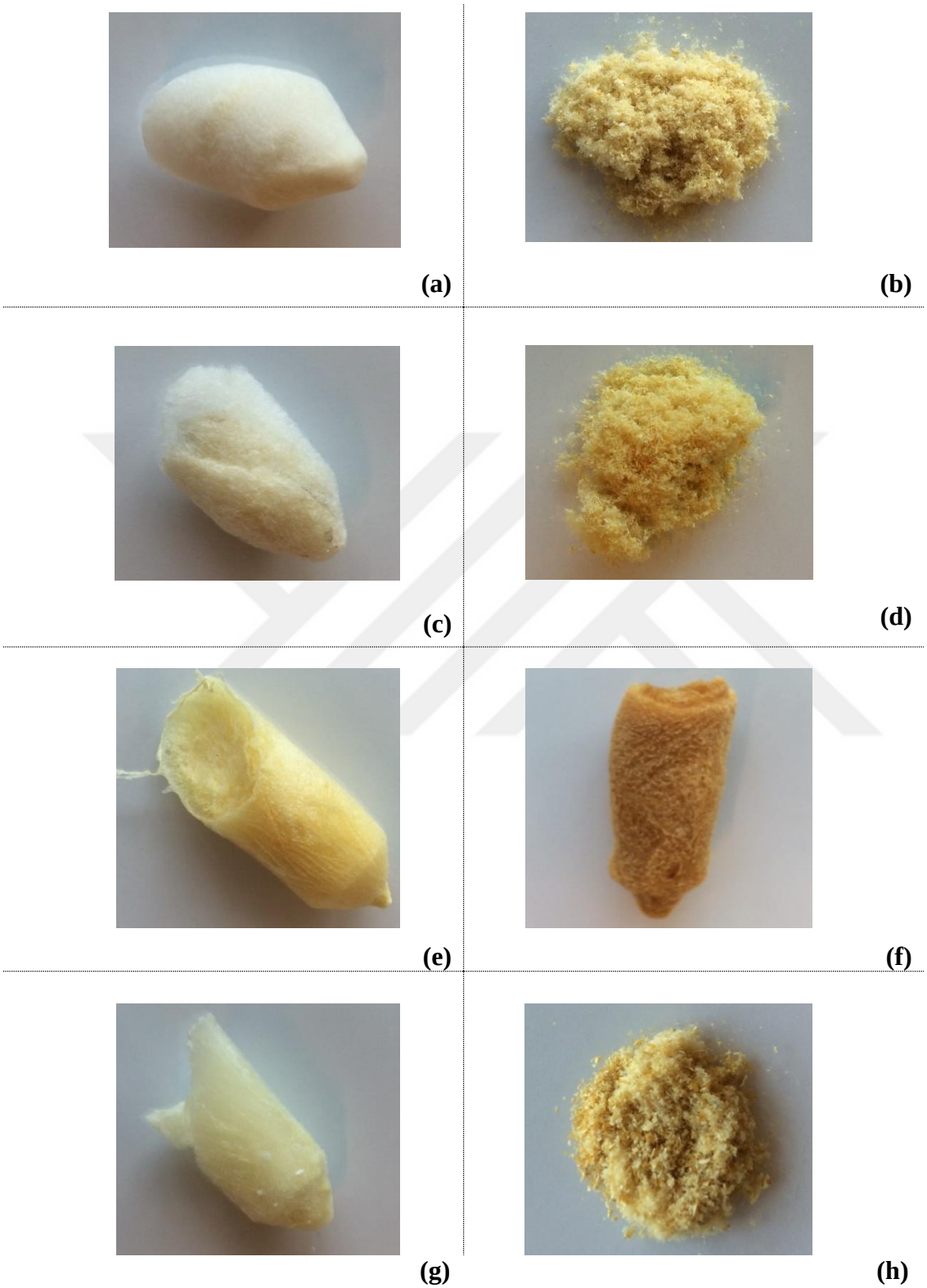

Figure A.1 : Appearance of dried formulations (a)IC-1v1. (b)CC-1v1. (c)IC-2v1. (d)CC-2v1. (e)IC-3v1. (f)CC-3v1. (g)IC-4v1 (h)CC-4v1

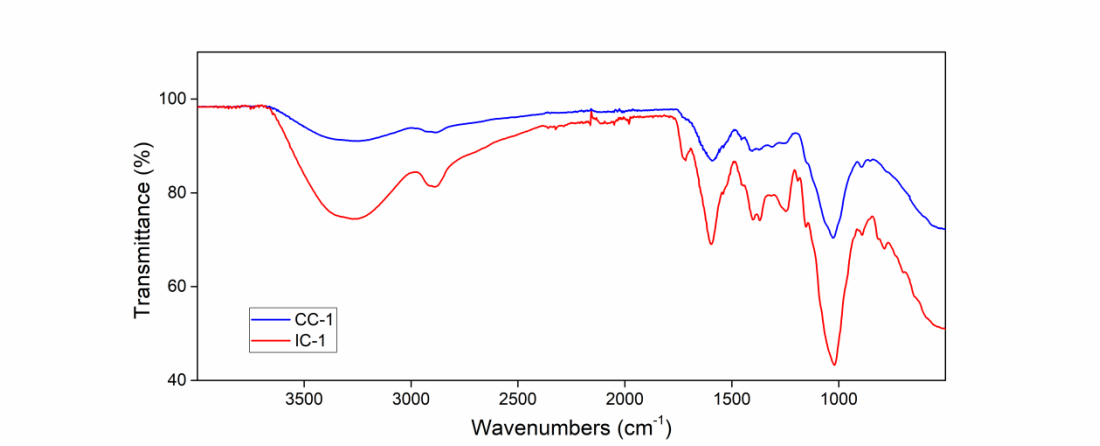

Figure A.2 : FTIR spectra of first version of empty CC-1v1 and IC-1v1

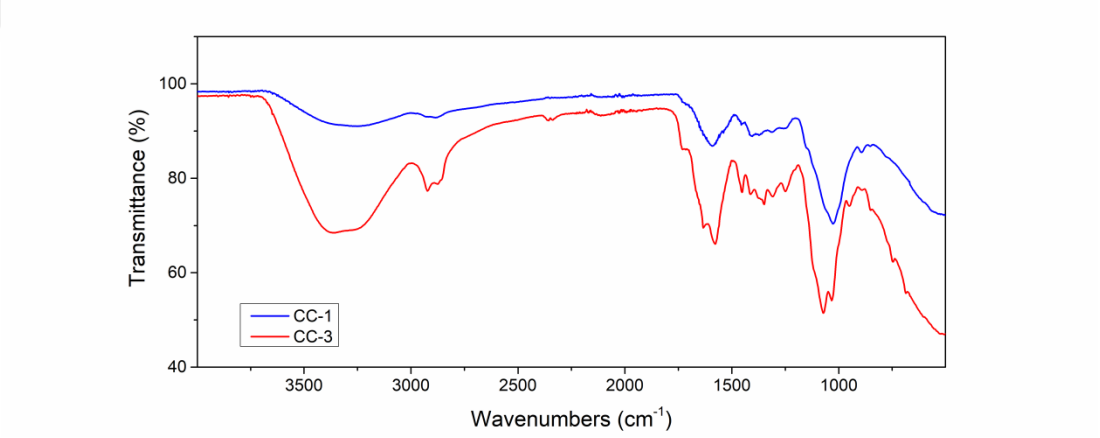

Figure A.3 : FTIR spectra of first version of empty CC-1v1 and TC loaded CC-3v1

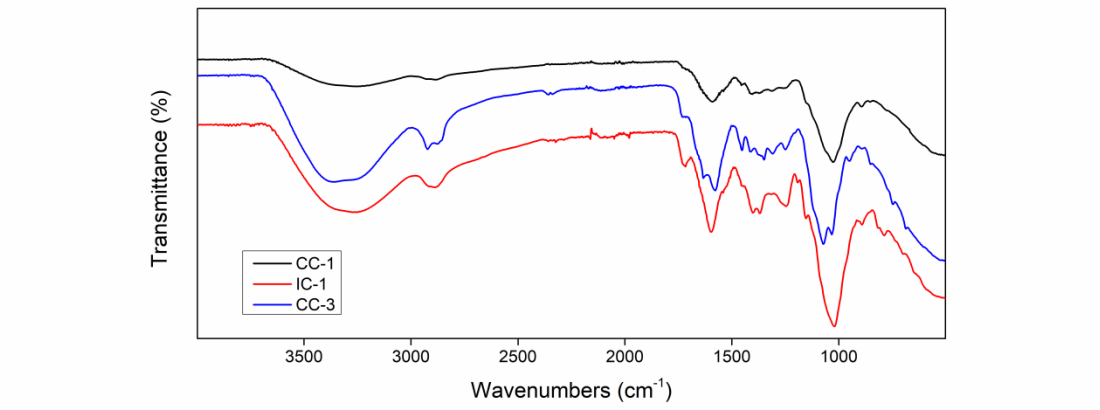

Figure A.4 : FTIR spectra of TC loaded CC-3v1 and its empty control groups

Table A.1 : Encapsulation efficiencies and loading capacities of all synthesized versions

Sample Name	Total TC SN (mg)	Added TC (mg)	Encapsulation Efficiency (%)	Initial Weight (mg)	After Drying (mg)	Loading Capacity (%)
IC-3v1	0.51368	350	99.8532	1050	970	36.0295
IC-4v1	1.57410	350	99.5502	1100	985	35.3731
CC-4v1	12.0792	350	96.548	1100	979	34.5169
IC-3v2	19.2927	160	87.9420	330	313	44.9543
IC-4v2	32.8117	160	79.4926	345	277	45.9163
CC-3v2	31.8920	160	80.0674	330	294	43.5741
CC-4v2	49.784	160	68.8844	345	256	43.0527

CURRICULUM VITAE

PHOTO

Name Surname **:** Taylan Baran Yeşil

EDUCATION **:**

- **B.Sc.** **:** 2018, Yıldız Technical University, Faculty of Chemisty and Metallurgy, Department of Bioengineering

PROFESSIONAL EXPERIENCE AND REWARDS:

- 2019-2022 Nanomik Biotechnology – Production Director
- 2018 University of Aveiro – Materials and Cell Laboratories Intern

PUBLICATIONS, PRESENTATIONS AND PATENTS ON THE THESIS:

- **T. B. Yesil, O. Guney** 2022: Encapsulation of Drug into Biopolymeric Matrices Based on Modified Xanthan Gum and Chitosan Microparticles, International Graduate Research Symposium IGRS'22, 1st th 3rd June 2022, İstanbul Turkey

OTHER PUBLICATIONS, PRESENTATIONS AND PATENTS:

- **B. B Orcen, T. B Yesil, A. Orcen, N. Aksoy, B. Ozcelik, E. Demircan, F. Marques, L. Coelho, I. Pinherio, J. Pimenta, O. Anuk, F. Altuner, F. N. Basaran** 2022: Controlling Lipid Oxidation by Microencapsulated Antioxidant, 4th International Symposium on Lipid Oxidation and Antioxidants, 23rd to 25th of May 2022, Vigo, Spain
- **M. Bjørge, C. R. Correia, T. B. Yesil, J. F. Mano** 2019: Patterned Discoidal Microfilms Modulate Osteogenic Differentiation, TERMIS EU 2019, 27th to 31st of May 2019, Rhodes, Greece
- **F. Çiftçi, A. Hacıoğlu, T.B. Yesil, C.B. Üstündağ** 2018: Designed and 3D Printed PLA Based Upper Extremity Finger Orthosis, Journal of Engineering Sciences and Design, vol.6, pp.460-463,24 September 2018